AD-A153 615 THE RESIDUAL STRENGTH OF CRACKED SPECIMENS REPRESENTING 1/1
A SECTION OF THE.. (U) AERONAUTICAL RESEARCH LABS
MELBOURNE (AUSTRALIA) A S MACHIN JUL 84
UNCLASSIFIED ARL-STRUC-R-408 F/G 1/3 NL

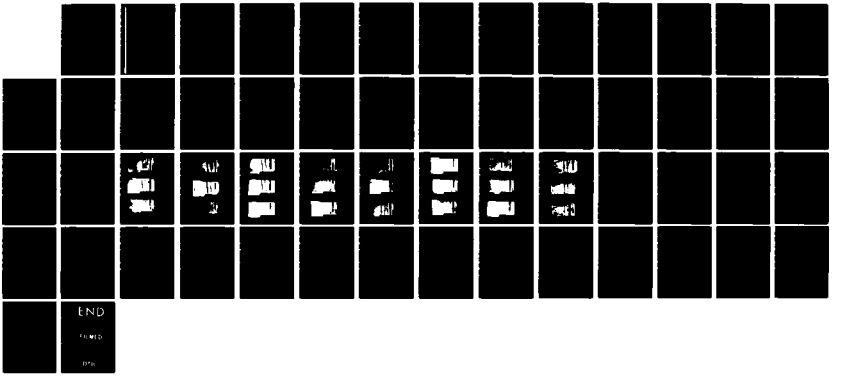

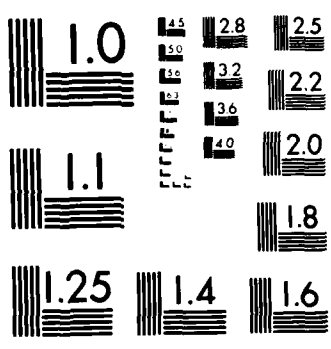

MICROCOPY RESOLUTION TEST CHART
NATIONAL BUREAU OF STANDARDS 1963 A

ARL-STRUC-R-408

AR-003-942

DEPARTMENT OF DEFENCE

DEFENCE SCIENCE AND TECHNOLOGY ORGANISATION

AERONAUTICAL RESEARCH LABORATORIES

MELBOURNE, VICTORIA

STRUCTURES REPORT 408

THE RESIDUAL STRENGTH OF CRACKED SPECIMENS REPRESENTING A SECTION OF THE MIRAGE IIIO WING MAIN SPAR

by

A. S. MACHIN

APPROVED FOR PUBLIC RELEASE

COPY No

JULY 1984

AR-003-942

DEPARTMENT OF DEFENCE
DEFENCE SCIENCE AND TECHNOLOGY ORGANISATION
AERONAUTICAL RESEARCH LABORATORIES

STRUCTURES REPORT 408

THE RESIDUAL STRENGTH OF CRACKED SPECIMENS REPRESENTING A SECTION OF THE MIRAGE IIIO WING MAIN SPAR

by

A. S. MACHIN

SUMMARY

The discovery of fatigue cracks at bolt holes in the wing main spar of many RAAF Mirage IIIO aircraft prompted an investigation into the residual strength of cracked specimens representing the critical section of the spar. Fatigue cracks were grown at the bolt holes of these specimens, which were frequently inspected to monitor the crack length. The specimens were then broken in static tension, the fracture surfaces photographed and the lengths, depths and areas of the fatigue cracks measured.

Using only the data available from the non-destructive inspection made just prior to the static failure it was not possible to predict accurately the specimen residual strength though it was possible to estimate a lower bound. Crack lengths, as estimated by the NDI technique used, were close to the measured crack lengths, though usually greater. Using the measured crack lengths, depths and areas it was not possible to predict accurately specimen residual strengths, though results were better than if information obtained only by NDI were used. Fracture mechanics techniques could not be used to predict residual strengths because of a lack of suitable Stress Intensity factor solutions.

POSTAL ADDRESS: Director, Aeronautical Research Laboratories,
Box 4331, P.O., Melbourne, Victoria, 3001, Australia

CONTENTS

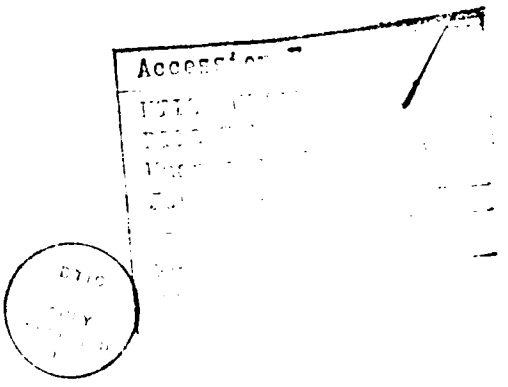

A-1

1. INTRODUCTION

The discovery of fatigue cracks at the innermost bolt holes along the lower rear flange of the wing main spar (Figs 1 and 2) in a large number of Mirage IIIO aircraft in the Royal Australian Air Force (RAAF) fleet prompted a comprehensive investigation (Refs 1 and 2) to explore methods for extending the spar fatigue life. The most critical section of the spar was the first bolt hole and associated single-leg-anchor-nut (SLAN) rivet holes; this section will be referred to in the remainder of this Report as the SLAN section.

Non-destructive inspections of the bolt hole at the SLAN section in service aircraft indicated a wide range of crack sizes, some of which were considered large enough to endanger the structural integrity of particular aircraft under normal operating conditions; consequently the normal operating *g* placards were reduced for these aircraft. However, if realistic loading limitations are to be imposed on in-service aircraft then information on the residual strength of the cracked structure is essential. In an attempt to provide this information a number of specimens (of the same type as used in the investigation reported in Refs 1 and 2) was fatigue tested until cracks of various sizes were developed at the first bolt hole, after which they were loaded statically until failure.

The results of this investigation and associated examinations of the fracture surfaces to provide information on the accuracy of the non-destructive inspection equipment used by the RAAF are given in this Report.

2. TEST MATERIAL AND SPECIMENS

Four batches of A7-U4SG* aluminium alloy plate procured by the RAAF were used for the manufacture of specimens. Details of the test material are as follows.

(i) *Batch 1* (ARL Serial No. GK)

One piece of 46 mm thick A7-U4SG-T651 plate measuring 854 mm wide by 2906 mm long.

(ii) *Batch 2A* (ARL Serial No. GN)

Four pieces of 48 mm thick A7-U4SG-T351† plate measuring 1250 mm wide by 500 mm long.

(iii) *Batch 2B* (ARL Serial No. GT)

Three pieces of 48 mm thick A7-U4SG-T351† plate measuring 1254 mm wide by 793 mm long.

(iv) *Batch 3* (ARL Serial No. GZ)

Three pieces of 55 mm thick A7-U4SG-T651 plate measuring 1000 mm wide by 2000 mm long.

---

* This is equivalent to the American aluminium alloy 2214.

† The specimens from Batches 2A and 2B were aged to the −T651 condition by heating to 160°C ±3°C for 20 hours immediately prior to the machining of the bolt and rivet holes.

The specimens (Fig. 3) were low-shear-load-transfer bolted joints designed to represent the spar flange at the critical location. They were taken from the plates with their longitudinal axes parallel to the rolling direction of the plates. After final failure some specimens from each material batch were used to provide tensile test specimens and compact tension fracture toughness specimens. The tensile specimens were taken from the test section of the parent fatigue specimens and the fracture toughness specimens (of 25 mm thickness) were manufactured from an end portion (Fig. 4). The slit plane of the fracture toughness specimens was perpendicular to the axis of the parent fatigue specimen, giving crack growth in the same direction as that of the fatigue crack in the fatigue specimens. The results of the tensile and compact tension fracture toughness tests, together with the chemical composition of the plates are given in Table 1.

The fatigue specimens were originally designed directly from drawings of the Mirage IIIO wing main spar. Subsequent detailed examination of spars from crashed aircraft and in-service wings (Ref. 3) indicated a number of discrepancies at the SLAN section between the actual spars and the drawings. The two most significant discrepancies were the use of 0·125 inch diameter 2117 aluminium alloy rivets instead of 2·5 mm diameter A-U4G aluminium alloy rivets to hold the SLAN and the tendency for the SLAN rivet holes to converge (at varying angles) towards the 8 mm bolt hole at the outer surface of the spar rather than be parallel to it, a condition referred to subsequently in this Report as 'inclined SLAN rivet holes'.

The discovery of inclined SLAN rivet holes in spars made the refurbishment of the SLAN section more difficult and considerably extended the life-enhancement program (Ref. 2). In the residual strength program two (TYPE 3 and TYPE 4) of the four inclined SLAN rivet hole configurations developed for the life enhancement program were used, in addition to specimens with parallel SLAN rivet holes. These three configurations are illustrated in Fig. 5, which also shows the numbering system for the holes at the SLAN section and indicates the orientation of this section of the specimen with respect to the Mirage wing main spar. All residual strength specimens but one (GK1E10), incorporated 0·125 inch 2117 aluminium alloy rivets.

3. SPECIMEN TESTING AND INSPECTION

Residual strength specimens were subjected to the same fatigue loading spectrum as the specimens used in the life-enhancement program. This spectrum was a simplified version (derived by Avions Marcel Dassault) of the Swiss Mirage full scale wing test spectrum. It was transformed into a 100-flight load sequence consisting of four different flight types (A', A, B, C) as illustrated in Fig. 6. Cycles of $+6{\cdot}5g/-1{\cdot}5g$ and $+7{\cdot}5g/-2{\cdot}5g$ (39 cycles in 100 flights) were applied at a cyclic frequency of 1 Hz, the remaining 1950 cycles were applied at 3 Hz; sine wave loading was adopted.

Fatigue loads on the specimens were based on the assumption that $+7{\cdot}5g$ corresponded to a *gross area* stress (not including the skin plate) of 180 MPa at the SLAN section and that there was a linear stress/g relationship, at $+7{\cdot}5g$ the testing machine load was nominally 404 kN. All fatigue loads were applied by a Tinius-Olsen servo-controlled electro-hydraulic fatigue machine, the 100-flight load sequence being achieved using an EMR model 1641 programmable function generator operating with punched tape.

There were 24 specimens used in this test program, of which 9 had inclined SLAN rivet holes. Nineteen of the 24 specimens were designated as residual strength specimens prior to any testing, the others were used in the residual strength program after, for example, machine controller failures. These five specimens will be discussed more fully in later paragraphs.

Each of the 19 specimens designated as residual strength specimens was subjected to at least 2000 flights of the fatigue loading sequence. The bolts were then removed and the bolt holes in the specimen inspected for cracks. Non-destructive inspections were performed at the Commonwealth Aircraft Corporation Ltd using a Förster Defectomat type F2-825* rotating probe eddy current hole inspection instrument. The specimen was then reassembled and, depending on the crack length detected in hole (1) and the crack length desired, either more

* Institut Dr Förster, Reutlingen, F.R. Germany.

flights of the fatigue sequence were applied or the specimen was set aside for static testing. Details of the numbers of flights applied and the crack lengths detected at hole (1) are contained in Table 2(*a*) (inclined SLAN rivet hole specimens) and Table 2(*b*), (parallel SLAN rivet hole specimens), in ascending order of residual strength. One residual strength specimen (GZ2D4) failed unexpectedly during the application of the fatigue sequence at the maximum of the peak load of the sequence.

Three parallel SLAN rivet specimens (GT2C, GZ3D10, GZ3A3), originally part of the life-enhancement program, were used as residual strength specimens after fatigue machine controller malfunctions resulted in extended periods of constant-amplitude cycling. The specimens were thus made invalid for their original purpose. The bolt holes in these specimens were inspected and at least 1000 flights of the normal fatigue sequence applied before static testing. Complete details are given in Table 2(*b*).

One specimen (GK1C9) which failed away from the SLAN section during the life-enhancement investigation was subsequently broken in static tension through the SLAN section and the result is given in Table 2(*b*). Additionally, specimen GK1E10, (a life-enhancement specimen that failed at the maximum of the peak load of the fatigue sequence) is included in Table 2(*b*) as an example of low residual strength. GK1E10 incorporated 2·5 mm A-U4G SLAN rivets, the only specimen mentioned in this Report to do so.

All specimens (except GZ2D4 and GK1E10) were broken in static tension in a 100 tonne Amsler Universal testing machine, the failure loads being recorded to an accuracy of 5 kN. As the 100 tonne Amsler was unavailable early in the residual strength program the first specimen used (GN4G) was repeatedly subjected to a static load of 600 kN (the maximum tensile capability of the Tinius–Olsen machine) between periods of fatigue loading under the 100-flight sequence.

4. DESCRIPTION OF FRACTURES

After static failure the lengths and depths of cracks originating at hole (1) were measured using a toolroom microscope (the measurement conventions adopted are shown in Fig. 7). Photographs (Fig. 8) were taken of all the fracture surfaces and these were used to determine, by graphical methods, the fatigue crack areas. This information is recorded in Table 3 (the specimens being in the same order as in Table 2) together with crack length estimates made using the Förster Defectomat prior to static testing, the failing load of each specimen and the failing load as a percentage of 890 kN. Unfortunately no uncracked specimens were tested in static tension, but 890 kN represents an estimate of the uncracked specimen failing load based on the static tensile data recorded in Table 1 and the strengths of specimens with small cracks.

As might be expected the extent of fatigue cracking affects the residual strength of the cracked specimen. For specimens which had a high residual strength, multiple small cracks are visible on the fracture surface at both the front and rear of hole (1). These cracks extend from about the midpoint of the section to the 'outer' or skin face of the specimen, e.g. specimens GT2D of Fig. 8(*a*) and GT1K of Fig. 8(*b*).

A reduction in specimen residual strength is associated with the development (by coalescence and increase in depth) of the multiple cracks along the bore of hole (1), leading to a larger crack at the rear of hole (1) than at the front. Small cracks are also evident along the bore of hole (2), e.g. specimens GZ2B2 of Fig. 8(*a*) and GZ3D10 of Fig. 8(*b*)*.

Finally, the fracture faces of specimens of low residual strength show the development of a large crack at the rear of hole (1) (often reaching the surface at the rear side of the specimen) and more extensive crack growth forward of hole (1) and along the bore of hole (2). For some specimens small cracks are apparent along the bore of hole (3), e.g. specimens GT3J of Fig. 8(*a*) and GK1E10 of Fig. 8(*b*).

---

* Crack development in the rivet holes during fatigue loading was not measured not only because it would have required the complete disassembly of the specimen, but also because no eddy-current probes of the appropriate size were available. Cracking associated with the SLAN rivet holes was not considered in the analysis of residual strength.

5. ANALYSIS AND DISCUSSION

Is it possible to estimate the static residual strength of a cracked specimen using only the information about the crack provided by NDI? A plot of total estimated crack length for each specimen (the sum of the length of all cracks, rear and forward, at hole (1) estimated using the Förster Defectomat) against residual strength (as a percentage of 890 kN) is shown in Fig. 9* and a plot of the estimated crack length at the rear of hole (1) (the larger crack) against residual strength in Fig. 10. Although these figures show that the residual strength tends to decrease as crack length increases they do not indicate a good correlation† between crack length (as estimated by NDI) and residual strength ($r^2 = 0{\cdot}56$ for Fig. 9, $r^2 = 0{\cdot}29$ for Fig. 10). Therefore, for a given estimated crack length it is not possible to make an accurate prediction of residual strength. Estimates of a lower bound to residual strength for a given crack length (as estimated by the present NDI method) can be made however. A boundary line may be drawn between the region of the Figure where failures have occurred and the region where no failures (in this investigation) have occurred and this line may be used to estimate a minimum residual strength. Alternatively, a line representing the lower limit of a confidence interval (derived from the regression analysis) may be drawn and used to estimate a minimum residual strength. In Figs 9 and 10 both a lower boundary line and the lower limit of the 95% confidence interval have been drawn.

An outcome of the present investigation is a check on the accuracy of crack measurements made using the equipment and techniques available to the RAAF. Figure 11 shows the relationship between individual fatigue crack lengths as estimated using the Förster Defectomat type F2-825 instrument prior to static failure and the actual fatigue crack lengths measured (after static failure) using a toolroom microscope. To aid interpretation of these data the line 'measured crack length = estimated crack length' is included.

Figure 11 shows that most crack lengths are overestimated when measured by this NDI technique, only five of the 39 points plotted indicate an underestimate of crack length. The 'best fit' curve to the data is a power curve with $r^2 = 0{\cdot}79$ and this shows that for estimated crack lengths up to about 16 mm the degree of overestimation of crack length using the NDI technique is small, e.g. for an estimated crack length of 8 mm the 'expected actual length' is 7 mm, for an estimated length of 16 mm the 'expected actual length' is 13·2 mm.

Increasing the accuracy of NDI estimates of crack length would allow more accurate predictions of specimen residual strength. Figure 12 is a plot of the sum (for each specimen) of the actual fatigue crack lengths front and rear of hole (1), measured using a toolroom microscope, against the residual strength (as a percentage of 890 kN) and Fig. 13 is a plot of the actual crack lengths at the rear of hole (1) against residual strength. The correlation coefficients are: $r^2 = 0{\cdot}75$ for Fig. 12 and $r^2 = 0{\cdot}67$ for Fig. 13. These correlation coefficients are an improvement on those for the data presented in Figs 9 and 10. They confirm that more accurate NDI estimates of crack length would allow more accurate prediction of specimen residual strength.

Using the 'best fit' curve to the data in Fig. 11 plots of 'expected actual length' against residual strength may be made. Figure 14 is analogous to Fig. 12—the sum (for each specimen) of the 'expected actual length' front and rear of hole (1) is plotted against the residual strength (as a percentage of 890 kN) and Fig. 15 is analogous to Fig. 13—the 'expected actual length' at the rear of hole (1) is plotted against residual strength. The correlation coefficients are: $r^2 = 0{\cdot}57$ for Fig. 14 and $r^2 = 0{\cdot}29$ for Fig. 15. These correlation coefficients are no better

---

* The data presented in Figs 9 to 20 are extracted from Table 3. The data from inclined SLAN rivet hole specimens (Table 3(*a*)) are plotted with a different symbol to that used for data from parallel SLAN rivet hole specimens (Table 3(*b*)), but no attempt has been made to analyze the results separately.

† First and second order polynomials were fitted to all data sets presented in Figs 9 to 19. In most cases the improvement in fit obtained by using a second order polynomial was not large. Additionally, third, fourth and fifth order polynomials and a power curve were fitted to the data presented in Fig. 18 and a power curve was fitted to the data presented in Fig. 11. Unless otherwise stated the correlation coefficients given in the text are for a first order fit to the data. See the Appendix.

than those for the data presented in Figs 9 and 10. Therefore there is no advantage in using the best fit curve to the data in Fig. 11 as a calibration curve for the crack lengths, as estimated by NDI, in making specimen residual strength predictions.

The non-destructive inspection technique used in this investigation (and by the RAAF) is not designed to measure crack depths. It is conceivable that a technique capable of making accurate crack depth measurements could be developed. Would such a technique increase the accuracy of residual strength predictions? Figure 16 is a plot of the sum (for each specimen) of the actual maximum crack depths front and rear of hole (1) against residual strength (as a percentage of 890 kN) and Fig. 17 is a plot of the crack depths at the rear of hole (1) against residual strength. The correlation coefficients are: $r^2 = 0{\cdot}78$ for Fig. 16 and $r^2 = 0{\cdot}72$ for Fig. 17. These correlation coefficients are very similar to those for the data presented in Figs 12 and 13. It appears that an accurate knowledge of the crack depth (used without other information) is no better than an accurate knowledge of crack length as a parameter for predicting residual strength.

If accurate crack depth and length measurements can be made it is likely that estimates may be made of crack areas. Figure 18 is a plot of total crack area (for each specimen) at hole (1) as a percentage of gross area against residual strength (as a percentage of 890 kN) and Fig. 19 is a plot of the crack area at the rear of hole (1) against residual strength. The correlation coefficients for a second order polynomial fit are: $r^2 = 0{\cdot}79$ for Fig. 18* and $r^2 = 0{\cdot}77$ for Fig. 19. These correlation coefficients are similar to (though greater than) those for the data presented in Figs 12 and 13 (crack length against residual strength) and similar to those for the data presented in Figs 16 and 17 (crack depth against residual strength). Thus it appears that the use of crack area as a predictor of residual strength will be little more accurate than the use of crack depth or crack length.

In each pair of plots discussed above the higher correlation coefficient has been for the case when information about cracks at the front and rear of hole (1) has been combined. This is expected, any cracking forward of hole (1) will affect residual strength and to consider cracking at the rear of the hole only is to disregard important information.†

The methods of Linear Elastic Fracture Mechanics (LEFM) can (with certain provisos) be used to predict the residual strength of cracked components (Ref. 4). However, to do so the crack configuration of the component must be accurately known and a stress intensity factor solution for the configuration obtained. The NDI technique used in this investigation cannot make quantitative crack depth measurements and so does not provide enough information to allow LEFM methods to be used to predict specimen residual strengths. On the assumption that an NDI technique capable of determining the crack configuration could be developed, a brief examination of some of the relevant literature (e.g. Refs 5, 6, 7) was made to see if applicable stress intensity factor solutions existed. None were found.

The residual strength information gathered in this investigation may be useful as a check on the accuracy of future stress intensity factor solutions for cracks from holes in thick sections. Specimen geometry, crack dimensions, failing load and material properties are known and are presented in this Report. It is likely that a finite element analysis would be more successful than a theoretical approach to the problem since crack shapes are irregular and the specimen geometry somewhat complex.

Unfortunately, with the present results there are no sets of specimens with very similar crack geometries. Such sets could be used to establish some measure of any scatter in residual strengths. Since linear elastic fracture mechanics depends on a knowledge of crack geometries information about the scatter in residual strengths of specimens with similar crack geometries would give some insight into the inherent accuracy limits of such information.

The cracks at hole (1) develop from multiple origins along the bore of the hole, as the fatigue life increases each crack grows and individual cracks coalesce (see Section 4). This type of crack

---

* The second order polynomial fitted to Fig. 18 is physically unrealistic since there is a minimum when the crack area is 7·6% of the gross area. Third, fourth and fifth order polynomial fits also have minimums. A power curve does not give as good a correlation coefficient as a second order polynomial.

† While preparing this report analysis of information only from cracks forward of hole (1) was performed, but correlation coefficients obtained using this information were poor.

extension results in a high, but variable, crack 'aspect ratio' (length/depth). Figure 20 is a plot of individual crack depths against length (measured after static failure). Included as part of this Figure are the lines 'length = 2 × depth' and 'length = 3 × depth' representing aspect ratios of 2 and 3 respectively. The majority of cracks with lengths of less than 14 mm have aspect ratios of greater than 4 and there is a large scatter in aspect ratios (mean aspect ratio = 5·74, standard deviation = 3·67). For cracks more than 14 mm long the aspect ratio is close to 3 and the scatter is sharply reduced (mean aspect ratio = 3·03, standard deviation = 0·38).

A possible reason for this change is that once the crack length exceeds about 14 mm the crack growth characteristics change. No longer does growth proceed by the formation and coalescence of multiple cracks along the hole bore, but instead crack growth occurs by the propagation of a single crack. If only one crack is present and no further cracks initiate then the relationship between crack length and depth (the 'aspect ratio') will be more stable.

6. CONCLUSIONS

A limited but potentially useful amount of information has been obtained from an investigation into the residual strength of cracked specimens representing a part of the lower rear flange of the main spar of the Mirage IIIO wing.

1. Knowledge of the NDI estimates of the crack length(s) in hole (1) of the specimen does not allow an accurate estimate of the specimen residual strength at this section to be made. However, a lower bound to residual strength may be predicted.

2. The non-destructive inspection equipment in use by the RAAF is capable of making acceptable estimates of the lengths of cracks in holes. The estimated crack lengths are usually greater than the actual crack lengths—a conservative error.

3. Increasing the accuracy of NDI crack length estimates would allow more accurate estimation of the specimen residual strength.

4. An accurate knowledge of crack depth or crack area (assuming the development of an NDI technique capable of providing this information) does not allow a better estimate of specimen residual strength than does an accurate knowledge of crack length.

5. Better estimates of specimen residual strength are possible when information about cracks at the front and rear of hole (1) is combined than when information only about cracks at the front or rear of the hole is used.

6. Since the NDI technique used in this investigation cannot determine crack geometry Linear Elastic Fracture Mechanics techniques cannot be used to make specimen residual strength predictions. If an NDI technique capable of determining crack geometry was developed a suitable stress intensity factor solution would have to be found.

7. ACKNOWLEDGEMENTS

The author expresses his appreciation to Mr W. F. Lupson of Structures Division of the Aeronautical Research Laboratories for his aid and co-operation during this investigation and also to Mr K. J. Coad of the Commonwealth Aircraft Corporation Ltd for carrying out frequent non-destructive inspections of the specimens used in this investigation.

The author also thanks Mr J. Y. Mann and Dr J. M. Finney of Structures Division of the Aeronautical Research Laboratories for many constructive comments during the writing of this Report.

REFERENCES

1. Mann, J. Y., Lupson, W. F., Machin, A. S., and Pell, R. A. Interim report on investigation to improve the fatigue life of the Mirage IIIO wing spar. *Aero. Res. Labs Structures Tech. Memo.* 334, August 1981.

2. Mann, J. Y., Machin, A. S., and Lupson, W. F. Improving the fatigue life of the Mirage IIIO wing main spar. *Aero. Res. Labs Structures Report* 398, January 1984.

3. Lupson, W. F., Mann, J. Y., and Harris, F. G. Examination of the inboard lower surface rear flange section of the main spars from six crashed Mirage IIIO aircraft wings. *Aero. Res. Labs Structures Tech. Memo.* 316, May 1980.

4. Use of linear elastic fracture mechanics in estimating fatigue crack growth rates and residual strengths of components. *ESDU Data Item* 80036, November 1980.

5. Newman, J. C., and Raju, I. S. Stress-intensity factor equations for cracks in three-dimensional finite bodies. *NASA Tech. Memo.* 83200, August 1981.

6. Rooke, D. P., and Cartwright, D. J. *Compendium of stress intensity factors.* London, HMSO, 1976.

7. Shah, R. C. Stress intensity factors for through and part through cracks originating at fastener holes. *Mechanics of crack growth.* ASTM STP 590, 1976, pp. 429–459.

APPENDIX

Regression Analyses

All regression analyses for this Report were performed on a Hewlett–Packard HP85 desk top computer using Hewlett–Packard supplied software.

The fitting of a curve to the data does not imply that a physical relationship of the same kind is expected.

FIGURE 9

A first order polynomial fit to the data gave the equation:

$$\% \text{ Residual strength} = 100 \cdot 76 - 1 \cdot 238 \text{ (total estimated crack length).}$$

$$r^2 = 0 \cdot 56$$

The lower limit of the 95% confidence interval is given by:

$$y = 88 \cdot 53 - 1 \cdot 770\, x$$

FIGURE 10

A first order polynomial fit to the data gave the equation:

$$\% \text{ Residual strength} = 95 \cdot 87 - 1 \cdot 534 \text{ (estimated crack length).}$$

$$r^2 = 0 \cdot 29$$

The lower limit of the 95% confidence interval is given by:

$$y = 78 \cdot 52 - 2 \cdot 70\, x$$

FIGURE 11

A power curve was considered to be a better fit than a first or second order polynomial, the equation was:

$$\text{measured crack length} = 1 \cdot 025 \text{ (estimated crack length)}^{0 \cdot 922}$$

$$r^2 = 0 \cdot 79$$

FIGURE 12

A first order polynomial fit to the data gave the equation:

$$\% \text{ Residual strength} = 101 \cdot 41 - 1 \cdot 566 \text{ (sum of measured crack lengths)}$$

$$r^2 = 0 \cdot 75$$

The lower limit of the 95% confidence interval is given by:

$$y = 92 \cdot 83 - 1 \cdot 977\, x$$

FIGURE 13

A first order polynomial fit to the data gave the equation:

$$\% \text{ Residual strength} = 104 \cdot 28 - 2 \cdot 694 \text{ (measured crack length)}$$

$$r^2 = 0 \cdot 67$$

The lower limit of the 95% confidence interval is given by:

$$y = 93 \cdot 17 - 3 \cdot 549\, x$$

FIGURE 14

A first order polynomial fit to the data gave the equation:

$$\% \text{ Residual strength} = 103 \cdot 0 - 1 \cdot 603 \text{ (sum of expected crack lengths)}$$

$$r^2 = 0 \cdot 57$$

The lower limit of the 95% confidence interval is given by:

$$y = 90 \cdot 28 - 2 \cdot 27\, x$$

FIGURE 15

A first order polynomial fit to the data gave the equation:

$$\% \text{ Residual strength} = 97 \cdot 88 - 2 \cdot 018 \text{ (expected crack length)}$$

$$r^2 = 0 \cdot 29$$

The lower limit of the 95% confidence interval is given by:

$$y = 79 \cdot 20 - 3 \cdot 536\, x$$

FIGURE 16

A first order polynomial fit to the data gave the equation:

$$\% \text{ Residual strength} = 91{\cdot}66 - 3{\cdot}887 \text{ (sum of measured crack depths)}$$

$$r^2 = 0{\cdot}78$$

The lower limit of the 95% confidence interval is given by:

$$y = 86{\cdot}1 - 4{\cdot}808\,x$$

FIGURE 17

A first order polynomial fit to the data gave the equation:

$$\% \text{ Residual strength} = 93{\cdot}38 - 6{\cdot}632 \text{ (measured crack depth)}$$

$$r^2 = 0{\cdot}72$$

The lower limit of the 95% confidence interval is given by:

$$y = 86{\cdot}64 - 8{\cdot}449\,x$$

FIGURE 18

A second order polynomial was considered to be a better fit than a first order polynomial, the equation is:

$$\% \text{ Residual strength} = 88{\cdot}38 - 11{\cdot}568 \text{ (total crack area)}$$

$$+ 0{\cdot}756 \text{ (total crack area)}^2$$

$$r^2 = 0{\cdot}79$$

The lower limit of the 95% confidence interval is given by:

$$y = 82{\cdot}87 - 16{\cdot}272\,x + 0{\cdot}168\,x^2$$

FIGURE 19

A second order polynomial was considered to be a better fit than a first order polynomial, the equation is:

$$\% \text{ Residual strength} = 87{\cdot}22 - 12{\cdot}411 \text{ (crack area)}$$

$$+ 0{\cdot}739 \text{ (crack area)}^2$$

$$r^2 = 0{\cdot}77$$

The lower limit of the 95% confidence interval is given by:

$$y = 80{\cdot}75 - 20{\cdot}904\,x - 0{\cdot}965\,x^2$$

TABLE 1

Properties of test material

(a) Chemical composition

*Specification A7-U4SG (2214) (%)	Plate batch serial No.			
	GK	GN	GT	GZ
Cu 3·9–5·0	4·56	4·40	4·26	4·43
Mg 0·2–0·8	0·38	0·33	0·35	0·36
Mn 0·4–1·2	0·62	0·60	0·66	0·62
Fe 0·30 max.	0·24	0·24	0·14	0·19
Si 0·5–1·2	0·73	0·77	0·73	0·72
Ti 0·15 max.	0·01	0·02	0·02	0·02
Cr 0·10 max.	Not analyzed			
Zn 0·25 max.				

(b) Static tensile

	*Specification A7-U4SG-T651 (2214-T651)	Plate batch serial No.			
		GK	GN	GT	GZ
0·1% proof stress (MPa)	—	440·5	444·7	449·5	450·8
0·1% proof stress (psi)		63,900	64,500	65,200	65,400
0·2% proof stress (MPa)	390	446·3	451·0	455·2	457·9
0·2% proof stress (psi)	56,600	64,700	65,400	66,000	66,400
Ultimate stress (MPa)	450	488·3	493·2	497·1	508·8
Ultimate stress (psi)	65,300	70,800	71,500	72,100	73,800
Elongation (%) $(5{\cdot}65\sqrt{A})$	5	10·1	12·3	11·4	11·5
0·1% PS/Ult	—	0·90	0·90	0·90	0·89

(c) Fracture toughness

	Plate batch serial No.								Pooled values (34 tests)	
	GK (10 tests)		GN (11 tests)		GT (5 tests)		GZ (8 tests)			
	Average	s.d.	Average	s.d.	Average	s.d.	Average	s.d.	Average	s.d.
$MPa.m^{\frac{1}{2}}$	30·3	0·5	33·2	1·2	32·4	1·8	32·0	0·5	31·9	1·5
$ksi.in.^{\frac{1}{2}}$	27·6	0·4	30·2	1·1	29·5	1·6	29·1	0·5	29·1	1·4

* *Conditions de controle des produits lamines en alliages d'aluminium utilises dans les constructions aerospatiales.* Ministere de la Defense, Direction Technique des Construction Aeronautiques AIR 9048, Edition No. 1, 26 December 1978, p. 91.

TABLE 2(a)

Inclined SLAN rivet hole specimens. Fatigue loading histories and crack lengths

Specimen number and type	Total flights	Crack lengths by NDI at hole (1) (mm)	
		Rear	Forward
GT20	3000	10	—
	4000	12	—
TYPE 3	4500	12·5	6
	5500	14	11
	6000	18·5	14
GT3J	4000	8	6
	5000	15·5	9·5
TYPE 3	5500	22·5	18·5
GZ2D9	2000	6	—
	2800	7	—
TYPE 4	3500	9	indication
	4000	11·5	4
	4300	11	6
	4700	13	7
GT3C	2000	1·5	—
	3000	5	—
TYPE 3	4000	6	—
	5000	12·5	5·5
	5500	12·5	7
	6000	14	10
GT3N	3000	indication	2
	4000	6	4
TYPE 3	5000	19·5	5·5
GZ2B2	2000	8	7·5, 2*
	2500	9·5	12
TYPE 4	3000	10	12
	3200	11	12·5

TABLE 2(a) (continued)

Inclined SLAN rivet hole specimens. Fatigue loading histories and crack lengths

Specimen number and type	Total flights	Crack lengths by NDI at hole (1) (mm)	
		Rear	Forward
GT2F	2300	7	—
	3300	8	—
TYPE 3	4300	9	—
GT2D	2500	5	—
	3000	12	2
TYPE 3			
GZ2A8	2000	—	—
	3000	4·5	—
TYPE 4	4000	14	—
	4500	9, 3*	—
	5000	8, 6·5*	—
	5300	16	2

* Two separate cracks detected.

TABLE 2(b)

Parallel SLAN rivet hole specimens. Fatigue loading histories and crack lengths

Specimen number	Total flights	Crack lengths by NDI at hole (1) (mm)	
		Rear	Forward
GK1E10	8542	no measurement	no measurement
GZ2D4	3000	11·5	6
	4000	14	8
	4500	14	9
	4900	16	11
	5342	no measurement	no measurement
GT1C	2700	—	—
	4000	—	—
	5000	7	3·5
	6000	10·5	4
	7000	16	11
GN4G	2500	—	—
	3500	—	—
	4500	6	—
	5500	9	—
	6500	15	5
	7000†	16	7
	7400	16	5
	7866†	17	7
	8345†	18	9
	8845†	19·5	10
	9345†	19·5	10
	9745†	25	11
	10 145	25	11
GT2C	unknown‡	9·5	6
	+1100	14	6·5
GZ3D10	unknown‡	8·5	4·5
	+1000	19	7
GT3M	3000	3·5	—
	5000	7	5
	5500	12·5	7
GZ2A12	3000	3·5	5
	4000	6·5	2·5
	5000	9·5	6
	5100	12	7·5
	6100	12	9

TABLE 2(b) (continued)

Parallel SLAN rivet hole specimens. Fatigue loading histories and crack lengths

Specimen number	Total flights	Crack lengths by NDI at hole (1) (mm)	
		Rear	Forward
GT1K	2500	—	—
	4000	2	—
	5000	7	—
	6000	8	6
GN3L	2000	8·5	—
	2500	9·5	—
GZ2B9	3000	7	—
	4000	9	—
	5000	11, 5·5*	7
	5500	17·5	7
GT3B	3000	4·5	—
	4000	4·5	—
	6000	7	—
	6500	8·5	6·5
	6900	9	6
GZ3A3	unknown‡	4	4·5
	+1000	7	6
GK1C9	7182	no measurement	no measurement
GN3D	2000	—	—
	2700	1·5	—
	3400	4·5	—
	3900	5·5	—
	4200	6	—
	5200	11	—
	6200	10·5	indication
	7000	10·5	indication
	7500	12·5	5

* Two separate cracks detected.
† Attempt to break specimen in a machine of 600 kN maximum capacity.
‡ Not known because of fatigue testing machine controller malfunction.

TABLE 3(a)

Inclined SLAN rivet hole specimens. Failing loads and crack dimensions at hole (1)

Specimen number and type	Failing load (kN)	Failing load as % of 890 kN	Pre-static failure crack length estimates (using Förster Defectomat)			Post-static failure crack parameter measurements (using microscope)			Fatigue cracked area as % of gross area
			Rear	Forward	Total	Rear	Forward	Total	
GT20	395	44	L 18·5	14	32·5	L 17·2 D 6·6	13·3 4·5	30·5 11·1	
TYPE 3						A 95	23·5	118·5	5·3
GT3J	465	52	L 22·5	18·5	41	L 16·3 D 4·8	11·3 3·9	27·6 8·7	
TYPE 3						A 57	19	76	3·4
GZ2D9	585	66	L 13	7	20	L 11·8 D 3·9	5·6 1·1	17·4 5·0	
TYPE 4						A 29	4·5	33·5	1·5
GT3C	605	68	L 14	10	24	L 12·9 D 2·2	10 1·2	22·9 3·4	
TYPE 3						A 17·5	5·5	23	1·0
GT3N	625	70	L 19·5	5·5	25	L 13·6 D 0·8	5·5 0·7	19·1 1·5	
TYPE 3						A 5	2	7	0·3
GZ2B2	640	72	L 11	12·5	23·5	L 10·2 D 2·6	11·3 2·3	21·5 4·9	
TYPE 4						A 15·5	14	29·5	1·3
GT2F	740	83	L 9	—	9	L 7·6 D 1·1	— —	7·6 1·1	
TYPE 3						A 6	—	6	0·3
GT2D	825	93	L 12	2	14	L 5·5 D 0·7	1·7 0·3	7·2 1·0	
TYPE 3						A 2	0·5	2·5	0·1
GZ2A8	845	95	L 16	2	18	L 8, 7* D 1·7, 1	2 0·4	17 2·1†	
TYPE 4						A 10, 4·5	0·5	15	0·7

L = crack length (mm) D = crack depth (mm) A = crack area (mm²)

* Two separate cracks.

† Sum of deeper crack at rear of hole (1) and crack forward of hole (1).

TABLE 3(b)

Parallel SLAN rivet hole specimens. Failing loads and crack dimensions at hole (1)

Specimen number	Failing load (kN)	Failing load as % of 890kN	Pre-static failure crack length estimates (using Förster Defectomat)			Post-static failure crack parameter measurements (using microscope)			Fatigue cracked area as % of gross area
			Rear	Forward	Total	Rear	Forward	Total	
GK1E10	405	46	L —	—	—	L 19 D 7 A 112	13 6 82	32 13 194	8·7
GZ2D4	405	46	L —	—	—	L 20·1 D 6·1 A 111	14·6 4·5 47	34·7 10·6 158	7·1
GT1C	425	48	L 16	11	27	L 16·1 D 6·3 A 73	9·6 3·6 22·3	25·7 9·9 95·3	4·3
GN4G	595	67	L 25	11	37	L 19 D 5·6 A 62	10·1 1·7 10	29·1 7·3 72	3·2
GT2C	610	69	L 14	6·5	20·5	L 11·5 D 3·2 A 28·5	5 1·2 4	16·5 4·4 32·5	1·4
GZ3D10	645	72	L 19	7	26	L 12·5 D 3·9 A 31	6·7 2·1 7·5	19·2 6 38·5	1·7
GT3M	670	75	L 12·5	7	19·5	L 12·8 D 2·2 A 14·5	4·2 0·5 1·5	17 2·7 16	0·7
GZ2A12	685	77	L 12	9	21	L 12 D 3 A 27	7·5 2·7 14	19·5 5·7 41	1·8
GT1K	720	81	L 8	6	14	L 12·2 D 3 A 6	8·5 2·7 1	20·7 5·7 7	0·3
GN3L	740	83	L 9·5	—	9·5	L 11 D 0·7 A 5·1	— — —	11 0·7 5·1	0·2

TABLE 3(b) (continued)

Parallel SLAN rivet hole specimens. Failing loads and crack dimensions at hole (1)

Specimen number	Failing load (kN)	Failing load as % of 890kN	Pre-static failure crack length estimates (using Förster Defectomat)			Post-static failure crack parameter measurements (using microscope)			Fatigue cracked area as % of gross area
			Rear	Forward	Total	Rear	Forward	Total	
GZ2B9	745	84	L 17·5	7	24·5	L 13·3 D 3·3 A 28	6·7 0·8 4	20 4·1 32	1·4
GT3B	745	84	L 9	6	15	L 7·9 D 2·0 A 12	5·8 0·4 1	13·7 2·4 13	0·6
GZ3A3	755	85	L 7	6	13	L 2·3 D 1·1 A 1	4·5 1·9 5	6·8 3·0 6	0·3
GK1C9	790	89	L —	—	—	L 4·5 D 1 A 4	— — —	4·5 1 4	0·2
GN3D	790	89	L 12·5	5	17·5	L 11·1 D 3·1 A 23	5 0·4 2	16·1 3·5 25	1·1

L = crack length (mm). D = crack depth (mm). A = crack area (mm^2).

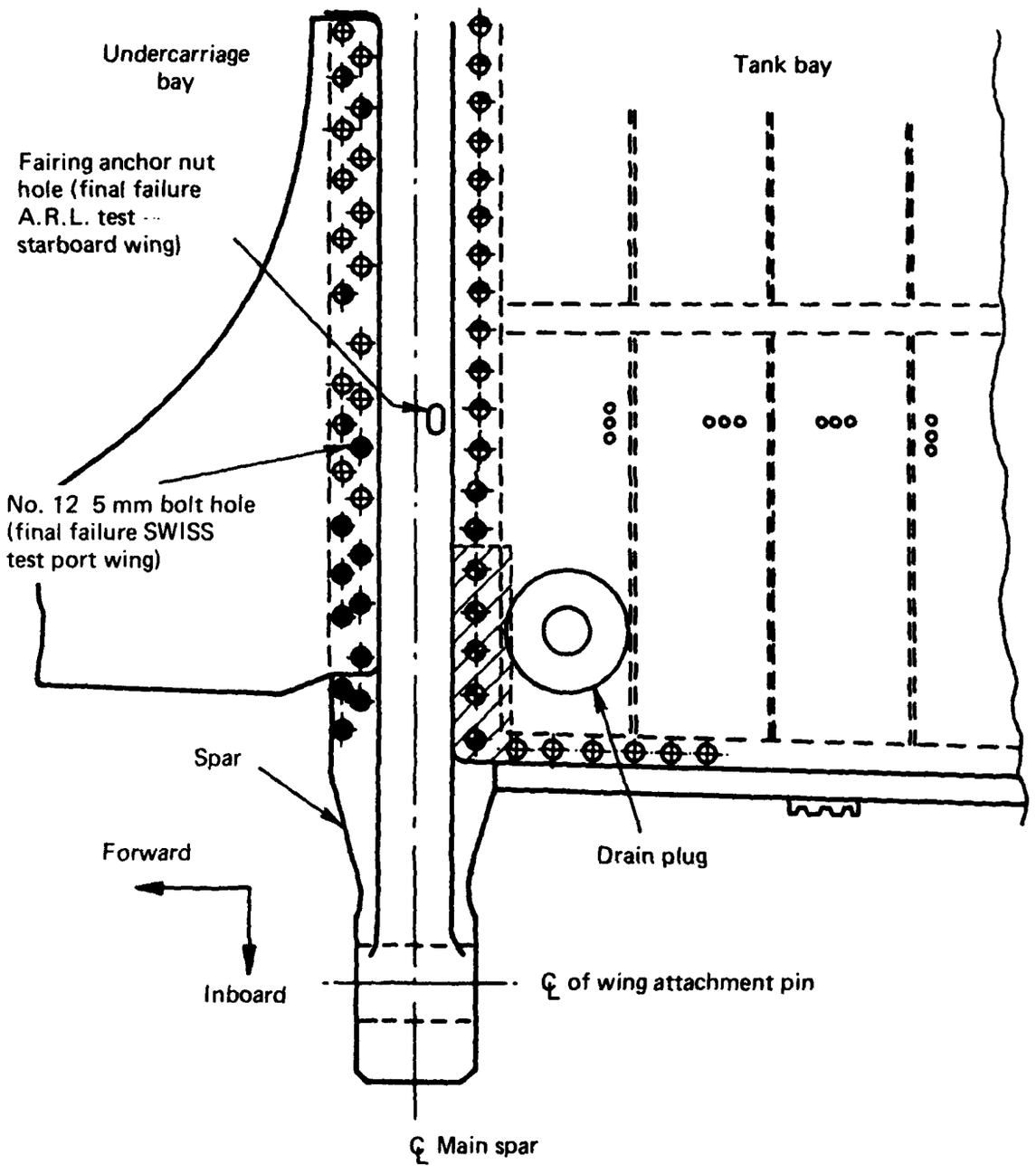

⊕	10 mm	hex.head shoulder bolt
⊕	8 mm	hex.head shoulder bolt
⊕	8 mm	countersunk head screw
⊕	6 mm	countersunk head screw
⊕	5 mm	hex.head bolt
⊕	5 mm	countersunk head bolt
⊕	Rivet	

Region of structure covered by this investigation

FIG. 1 MIRAGE PORT WING VIEWED FROM LOWER SURFACE

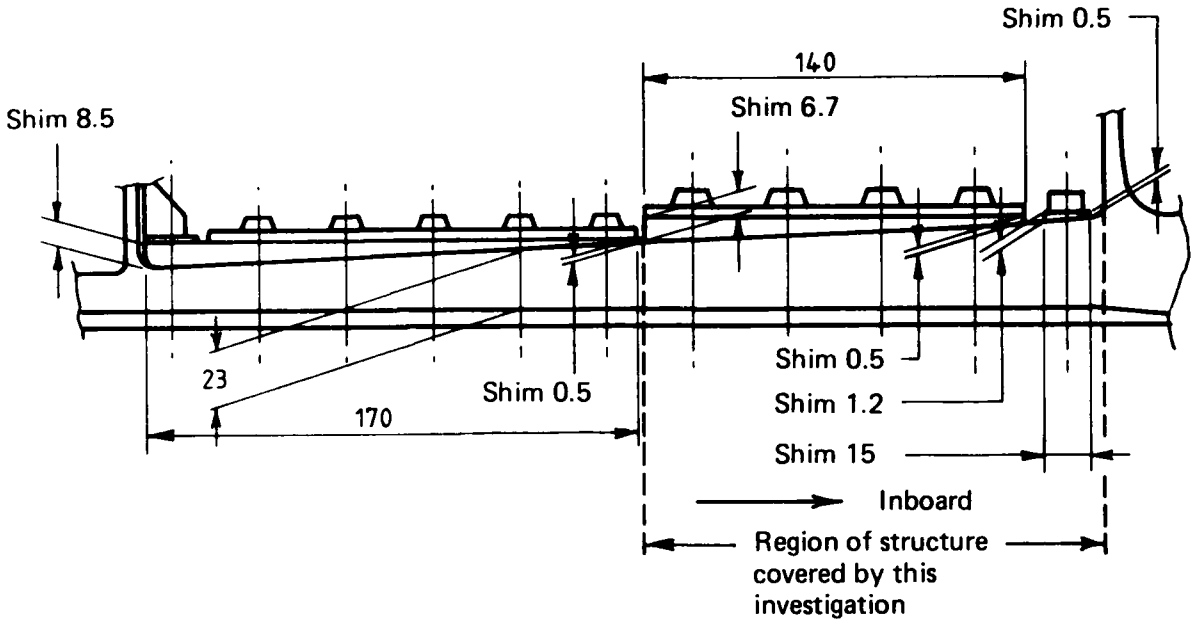

Legend

- 10 mm dia. shoulder bolt (8 x 1.25 thread) MIR. IIIC – 110.058
- 8 mm dia. shoulder bolt (6 x 1 thread) MIR. IIIC – 110.055
- 3 mm dia. countersunk head rivet (A-U4G)
- 2.5 mm dia. countersunk head rivet (A-U4G)

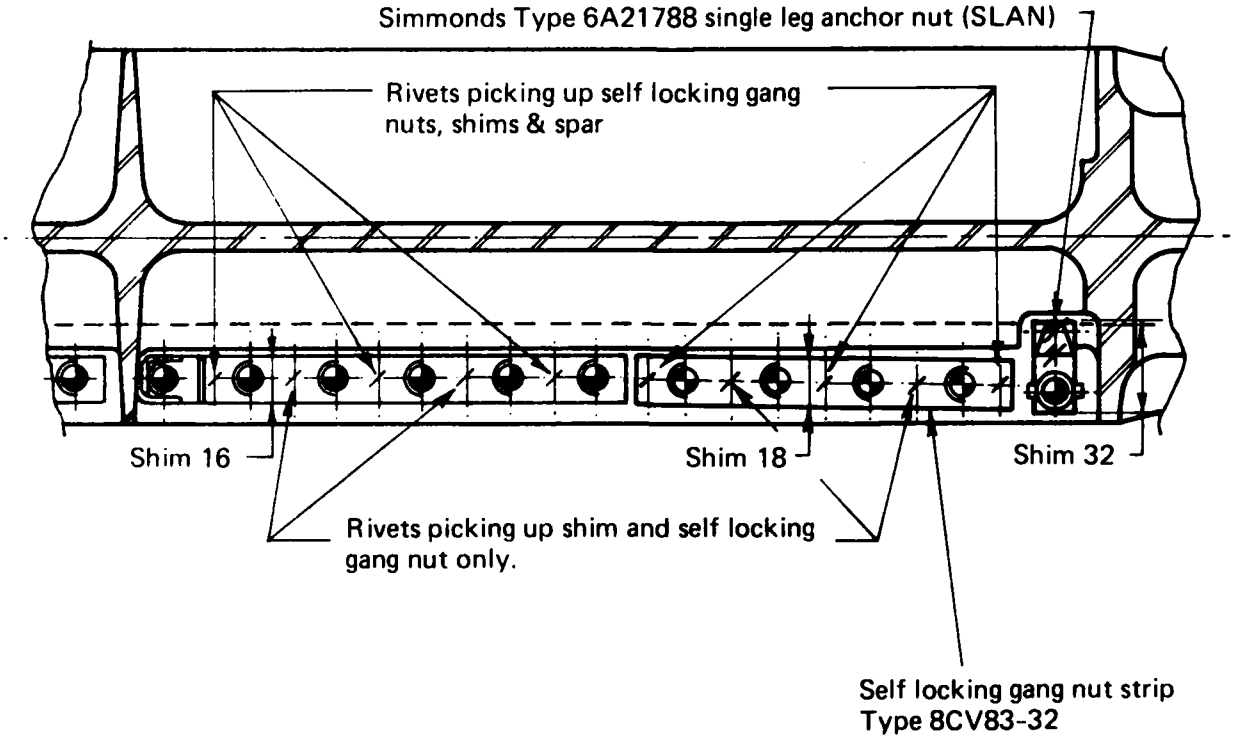

All dimensions in mm

Taken from AMD Manufacturing Drawing No. MIR.IIIE-113/2

FIG. 2 MAIN SPAR LOWER SURFACE, REAR FLANGE DETAIL.

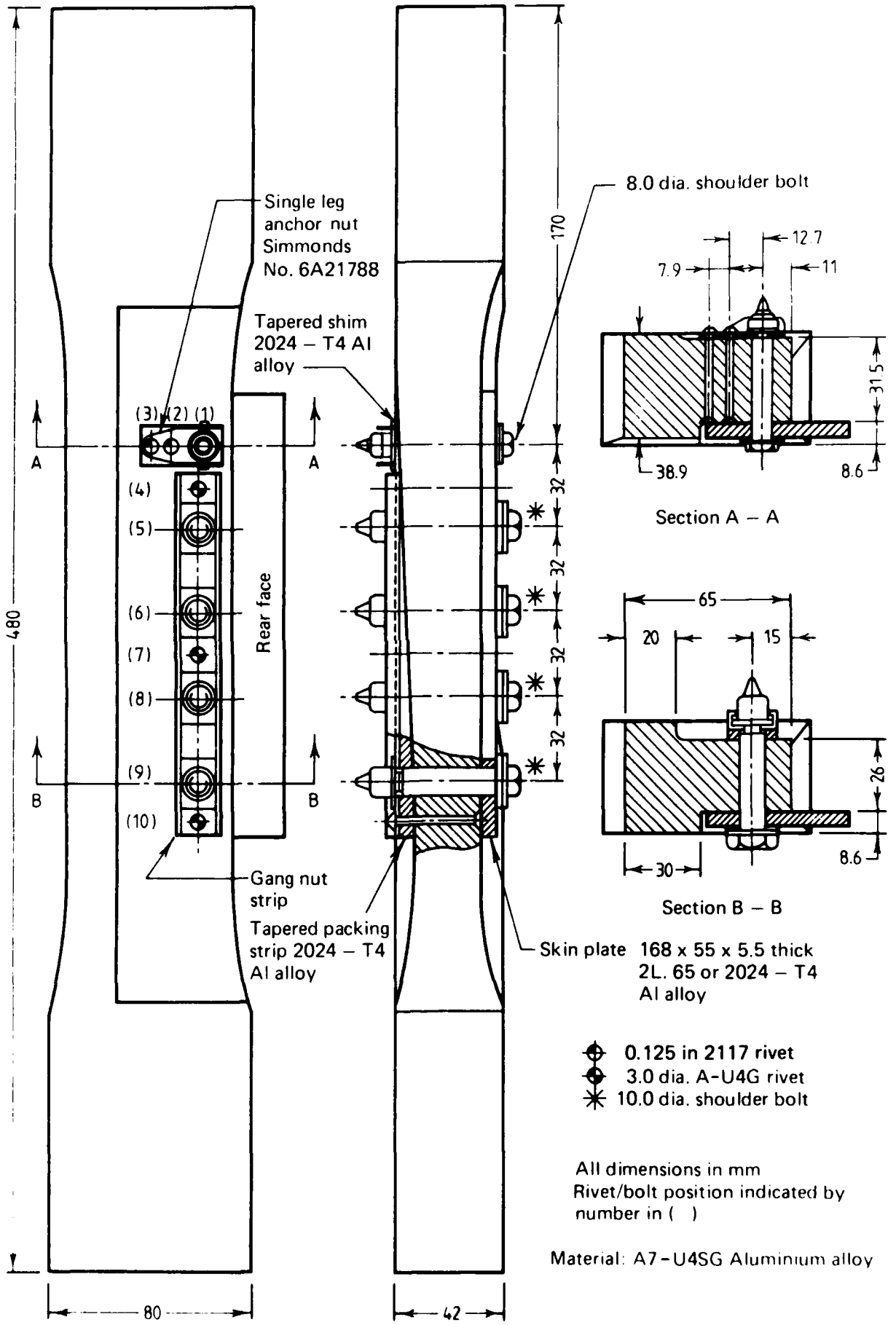

FIG. 3 MIRAGE SPAR LOWER REAR FLANGE FATIGUE SPECIMEN

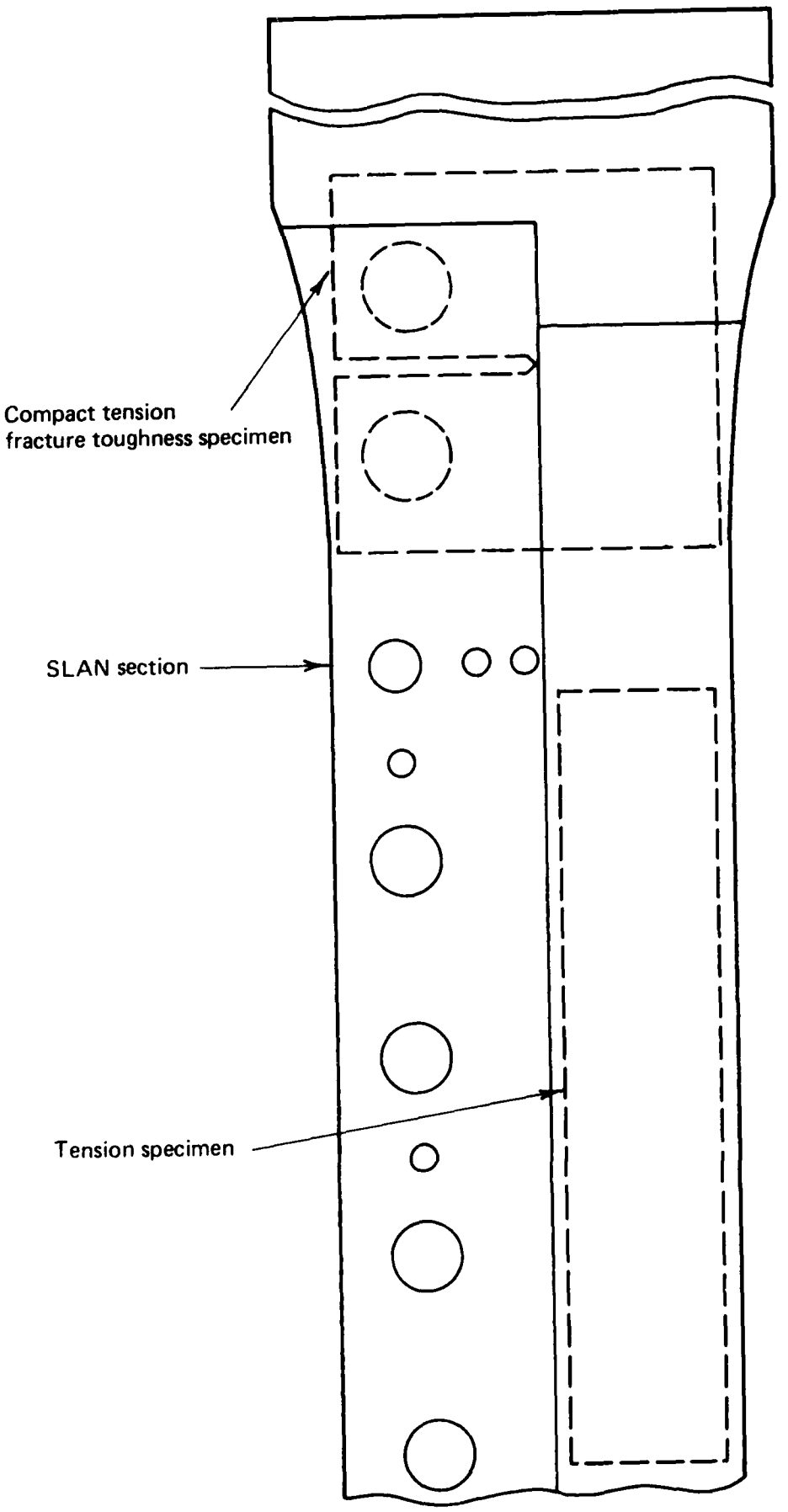

FIG. 4 LOCATIONS OF TENSION AND FRACTURE TOUGHNESS SPECIMENS

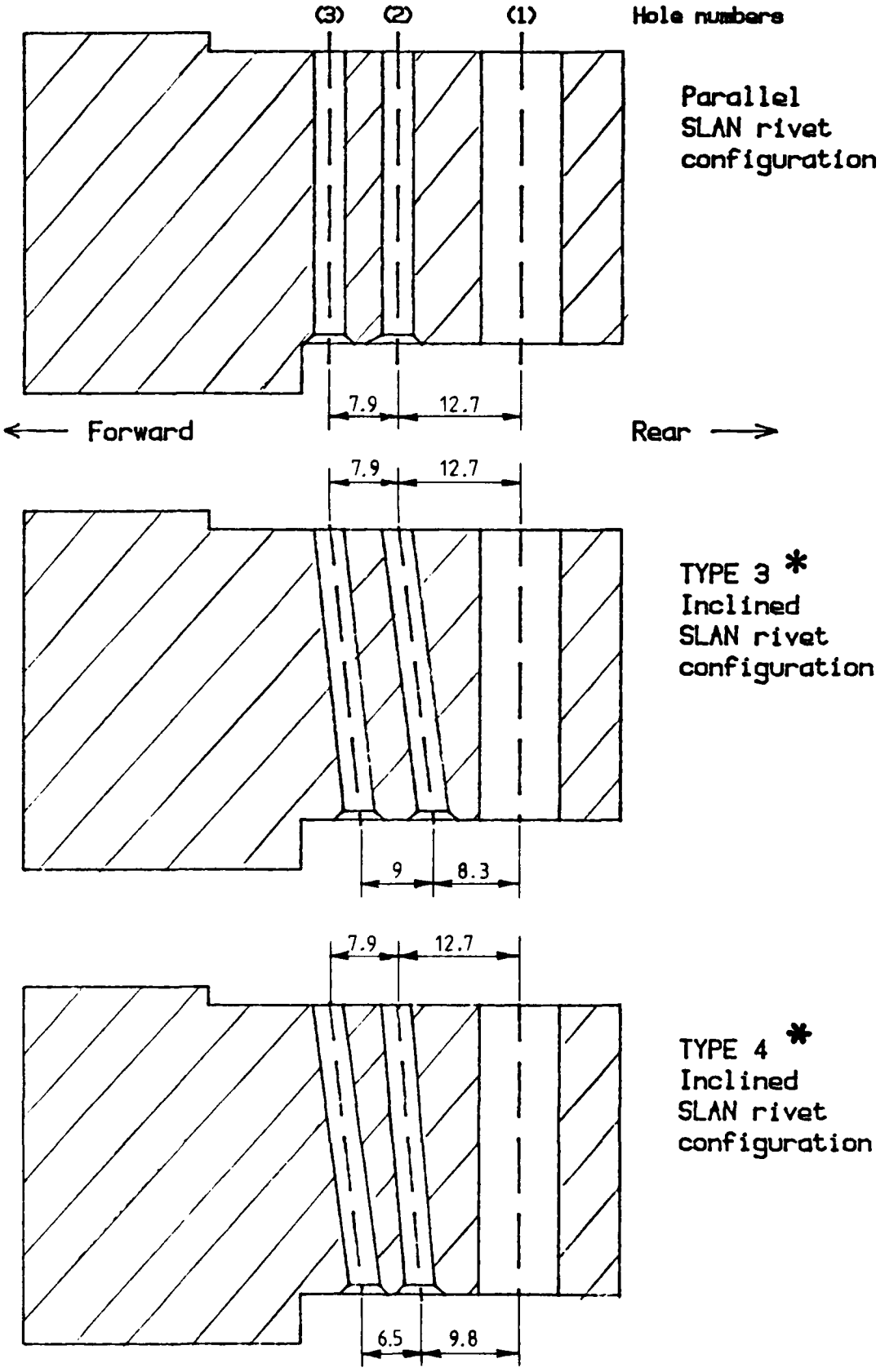

All dimensions in mm

* Inclined SLAN rivet configurations designated in accordance with practise of Ref. 2

FIG. 5 SPECIMEN SLAN SECTIONS

100 FLIGHTS (1989 CYCLES) REPRESENT 66.6 HOURS OF FLYING

FLIGHT A' →	10 CYCLES +3g/+1g	5 CYCLES +4g/+0.5g	2 CYCLES +5g/0g	1 CYCLE +6.5g/-1.5g	1 CYCLE +7.5g/-2.5g	1 CYCLE +6.5g/-1.5g	2 CYCLES +5g/0g	4 CYCLES +4g/+0.5g	10 CYCLES +3g/+1g

FLIGHT A →	10 CYCLES +3g/+1g	2 CYCLES +4g/+0.5g	2 CYCLES +5g/0g	2 CYCLES +6.5g/-1.5g	2 CYCLES +5g/0g	2 CYCLES +4g/+0.5g	5 CYCLES +3g/+1g

FLIGHT B →	5 CYCLES +3g/+1g	5 CYCLES +4g/+0.5g	9 CYCLES +5g/0g	4 CYCLES +4g/+0.5g	5 CYCLES +3g/+1g

CYCLES OF +6.5g/-1.5g AND
+7.5g/-2.5g AT 1 Hz;
REMAINDER OF CYCLES AT 3 Hz

FLIGHT C →	5 CYCLES +3g/+1g	1 CYCLE +4g/+0.5g	5 CYCLES +3g/+1g

SEQUENCE OF FLIGHTS IN 100 FLIGHTS: 1 FLIGHT A', 18 FLIGHTS A, 36 FLIGHTS B AND 45 FLIGHTS C

1	2	3	4	5	6	7	8	9	10	11	12	13	14	15	16	17	18	19	20	21	22	23	24	25	26	27	28	29	30	31	32	33	34	35	36	37	38	39	40	41	42	43	44	45	46	47	48	49	50
B	C	C	B	C	C	C	A	C	C	B	B	A	C	C	C	B	A	C	B	B	B	A	C	C	C	A	A	C	C	B	B	B	C	B	A	B	C	C	B	A	A'	B	C	C	A	A	B	B	C
51	52	53	54	55	56	57	58	59	60	61	62	63	64	65	66	67	68	69	70	71	72	73	74	75	76	77	78	79	80	81	82	83	84	85	86	87	88	89	90	91	92	93	94	95	96	97	98	99	100
C	B	C	C	B	C	B	B	C	C	C	A	B	A	C	C	C	B	A	B	B	B	C	B	C	C	A	B	C	B	A	B	C	C	B	A	A	B	C	C	B	C	C	B	B	C	B	C	A	C

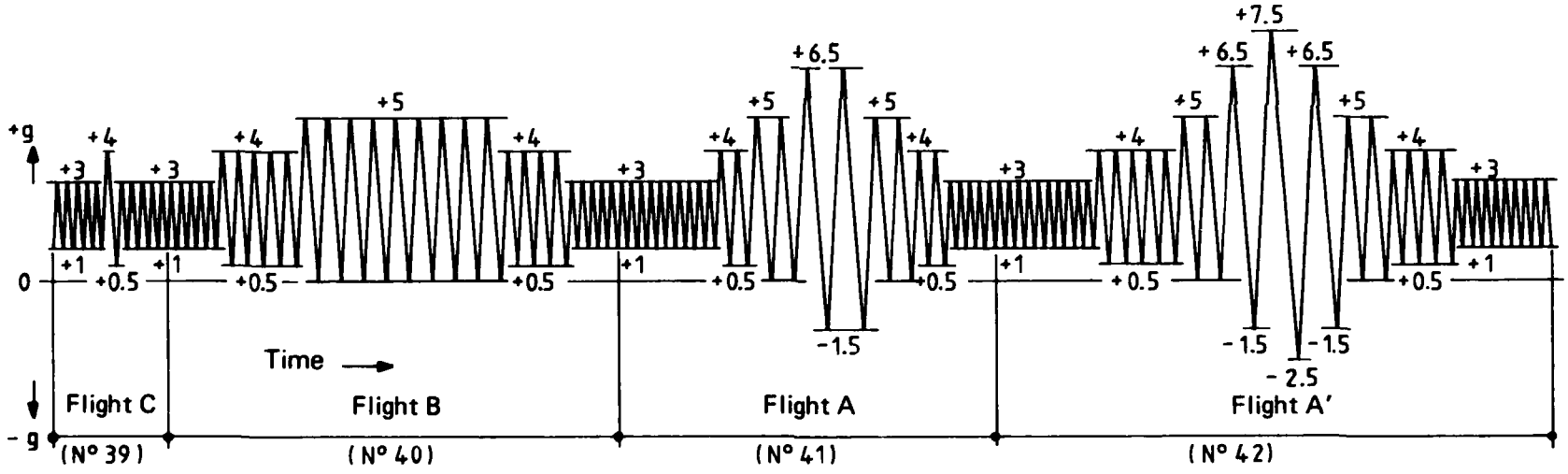

FIG. 6 FRENCH 100 FLIGHT MIRAGE III FLIGHT-BY-FLIGHT SEQUENCE

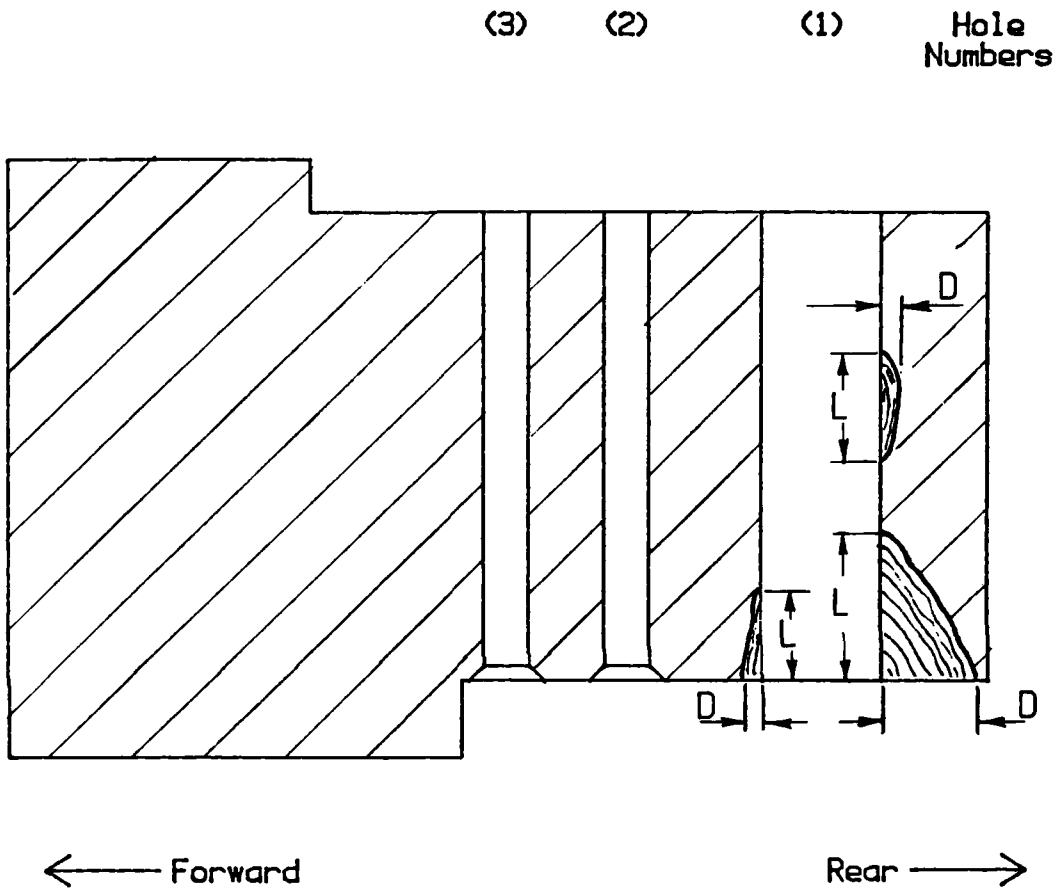

L = crack length

D = crack depth

FIG. 7 CRACK MEASUREMENT CONVENTIONS

GT2O
Type 3 specimen

Flights
applied: 6000

Failing
load: 395 kN

GT3J
Type 3 specimen

Flights
applied: 5500

Failing
load: 465 kN

GZ2D9
Type 4 specimen

Flights
applied: 4700

Failing
load: 585 kN

FIG. 8(a) FRACTURE SURFACES OF INCLINED SLAN RIVET HOLE STATIC RESIDUAL STRENGTH SPECIMENS ARRANGED IN ORDER OF INCREASING RESIDUAL STRENGTHS.

GT3C
Type 3 specimen
Flights applied: 6000
Failing load: 605 kN

GT3N
Type 3 specimen
Flights applied: 5000
Failing load: 625 kN

GZ2B2
Type 4 specimen
Flights applied: 3200
Failing load: 640 kN

FIG. 8(a) CONTINUED

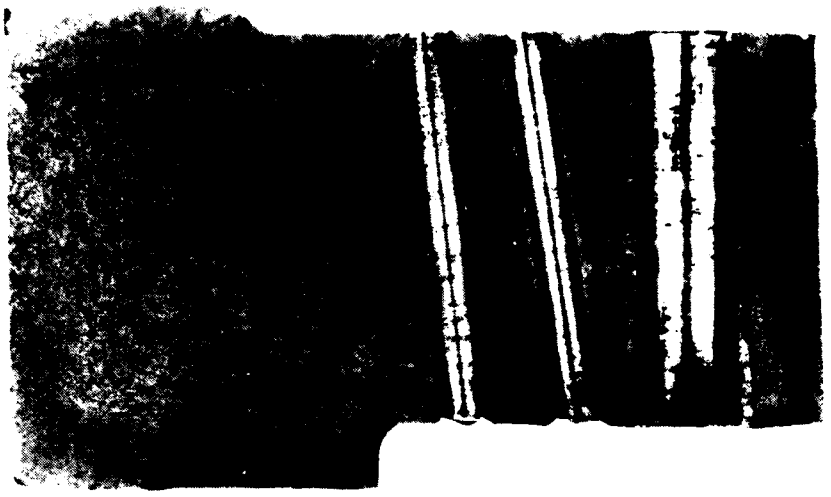

GT2F
Type 3 specimen

Flights
applied: 4300

Failing
load: 740 kN

GT2D
Type 3 specimen

Flights
applied: 3000

Failing
load: 825 kN

GZ2A8
Type 4 specimen

Flights
applied: 5300

Failing
load: 845 kN

FIG. 8(a) CONTINUED

GK1E10

Flights applied: 8542

Failing load: 405 kN

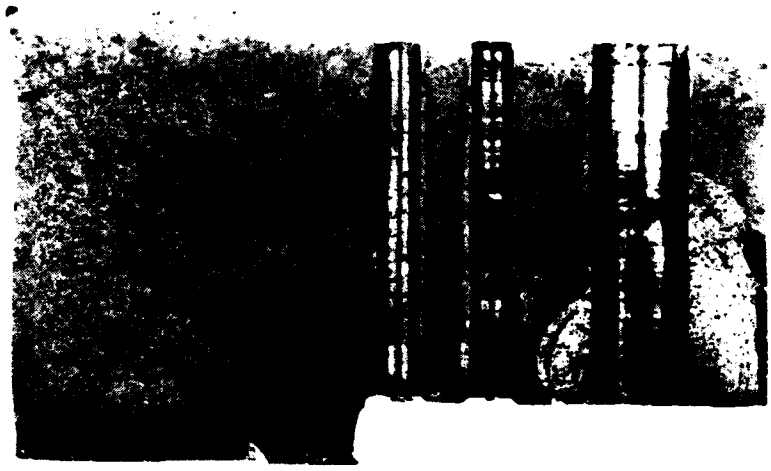

GZ2D4

Flights applied: 5342

Failing load: 405 kN

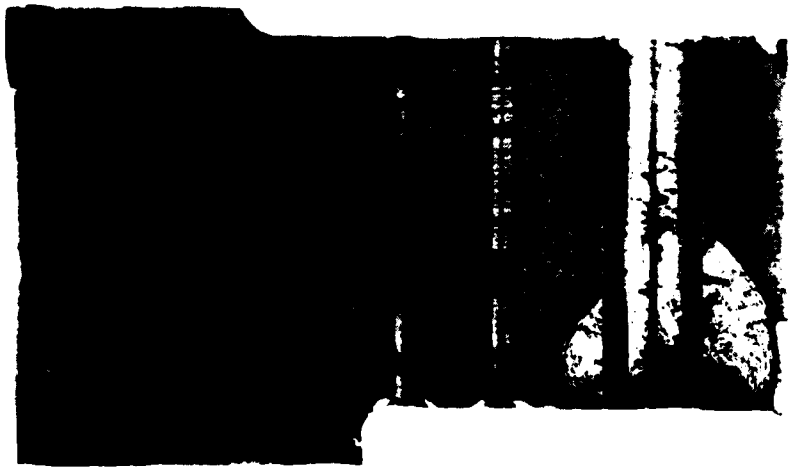

GT1C

Flights applied: 7000

Failing load: 425 kN

FIG. 8(b) FRACTURE SURFACES OF PARALLEL SLAN RIVET HOLE STATIC RESIDUAL STRENGTH SPECIMENS ARRANGED IN ORDER OF INCREASING RESIDUAL STRENGTHS.

GN4G

Flights applied: 10145

Failing load: 595 kN

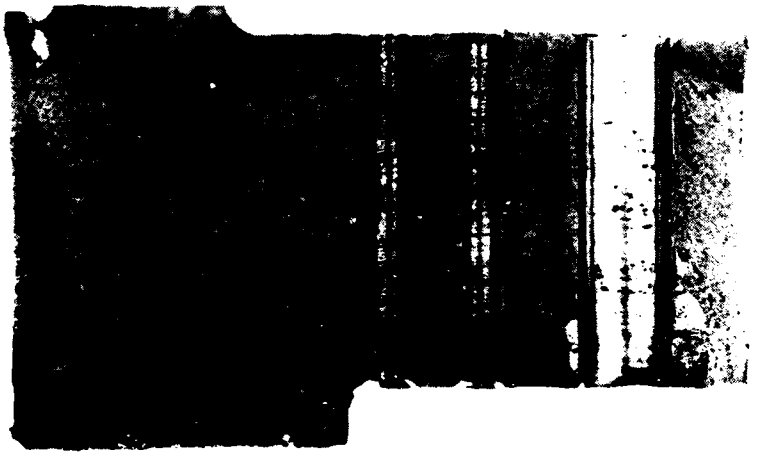

GT2C

Flights applied: not recorded.

Failing load: 610 kN

GZ3D10

Flights applied: not recorded.

Failing load: 645 kN

FIG. 8(b) CONTINUED

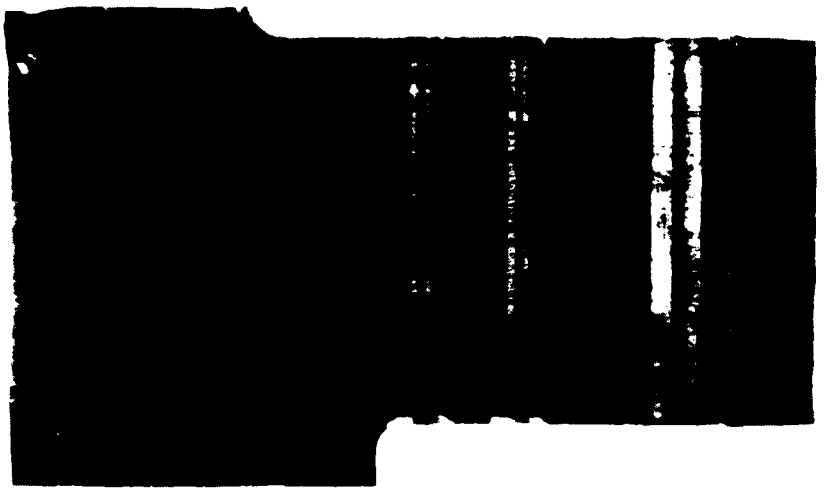

GT3M

Flights applied: 5500

Failing load: 670 kN

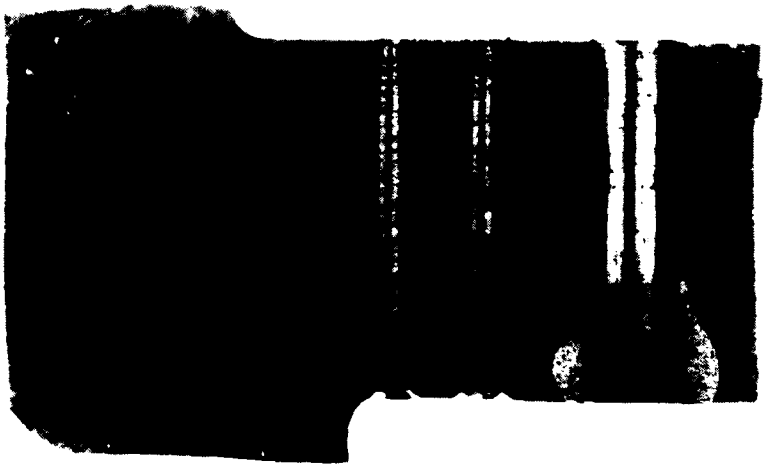

GZ3A12

Flights applied: 6100

Failing load: 685 kN

GT1K

Flights applied: 6000

Failing load: 720 kN

FIG. 8(b) CONTINUED

GN3L

Flights applied: 2500

Failing load: 740 kN

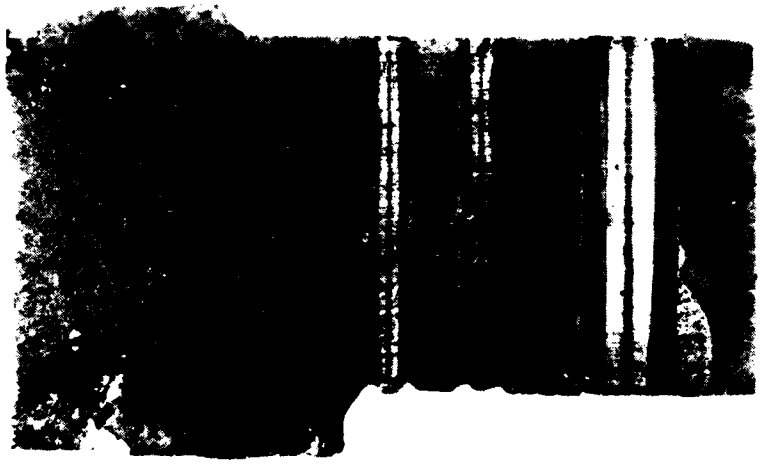

GZ2B9

Flights applied: 5500

Failing load: 745 kN

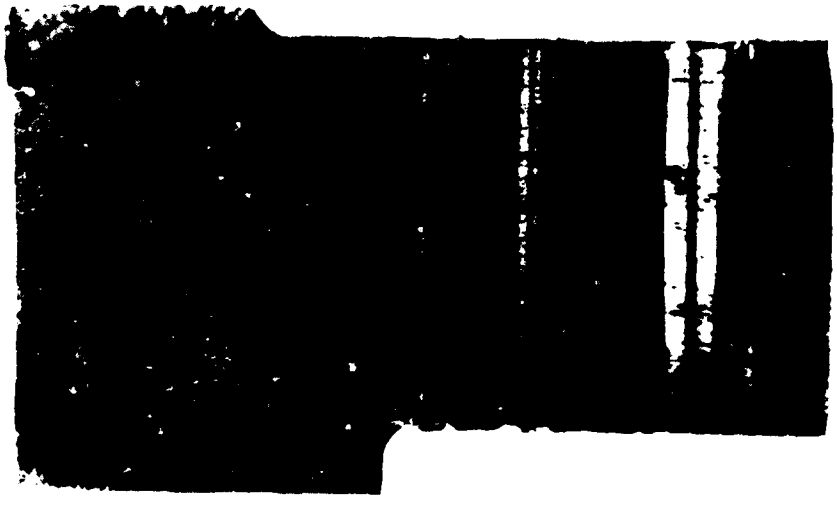

GT3B

Flights applied: 6900

Failing load: 745 kN

FIG. 8(b) CONTINUED

GZ3A3

Flights applied: not recorded.

Failing load: 755 kN

GK1C9

Flights applied: 7182

Failing load: 790 kN

GN3D

Flights applied: 7500

Failing load: 790 kN

FIG. 8(b) CONTINUED

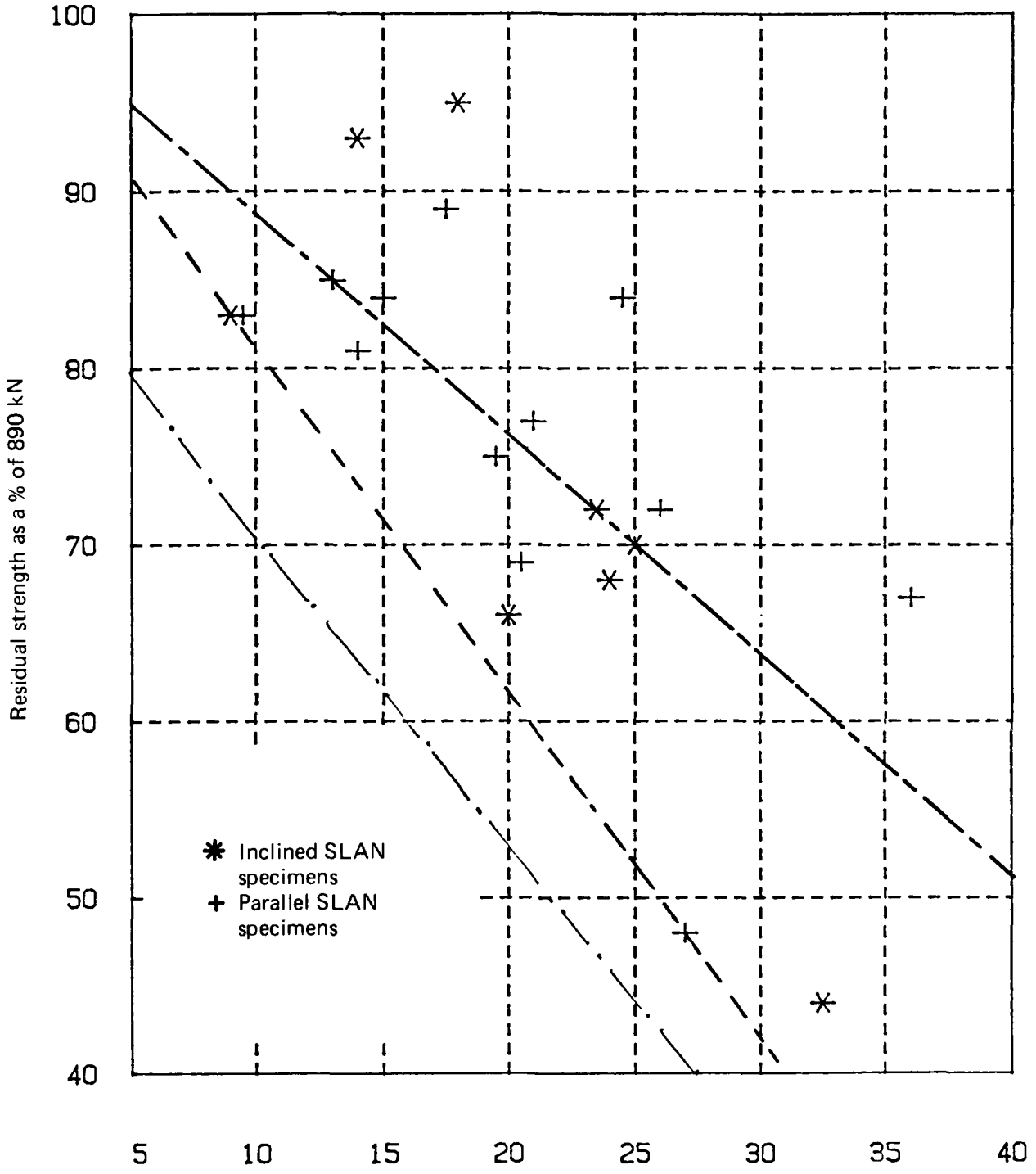

FIG. 9 SPECIMEN RESIDUAL STRENGTH vs SUM OF NDI ESTIMATES OF CRACK LENGTHS FRONT AND REAR OF HOLE (1)

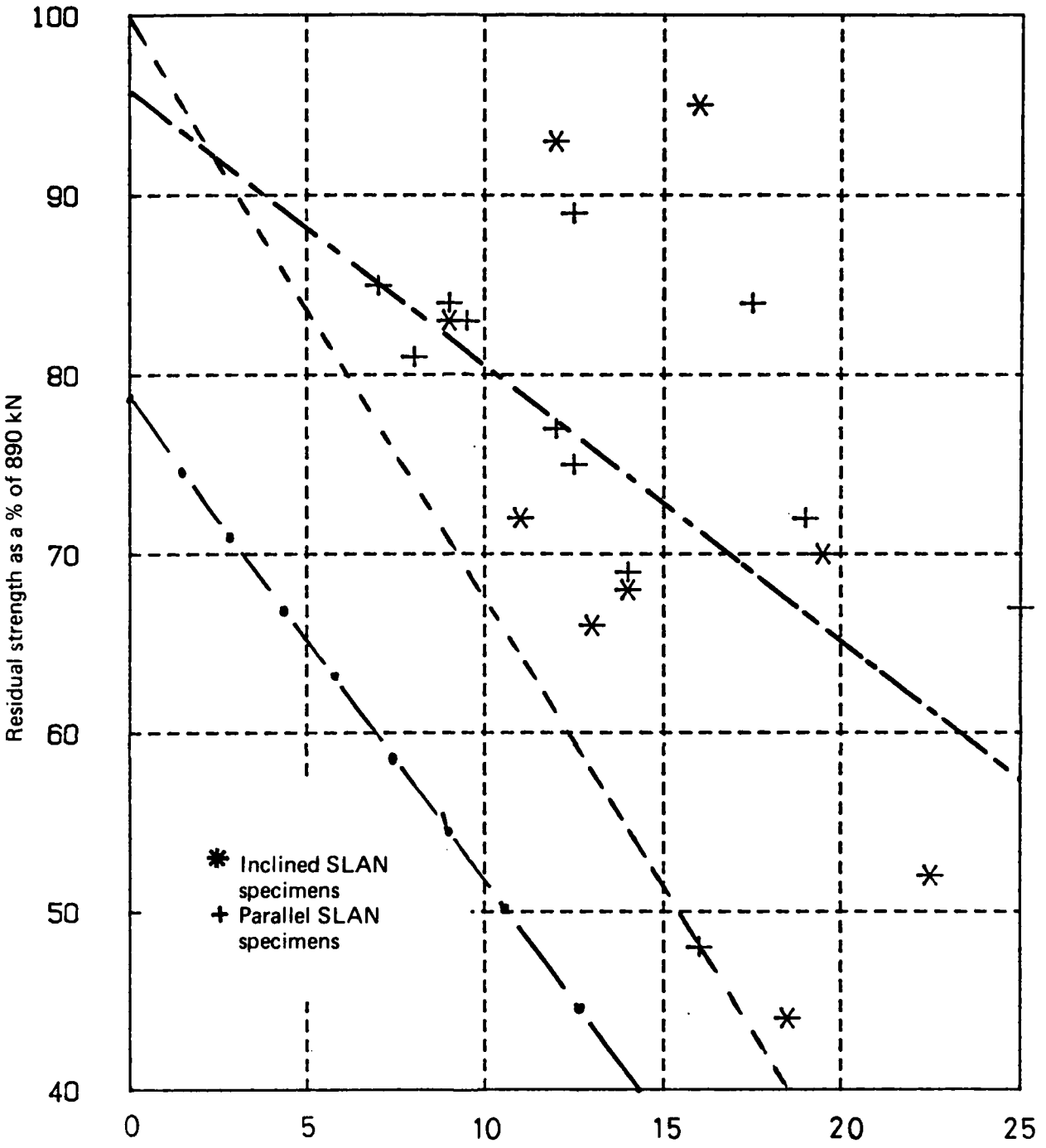

FIG. 10 SPECIMEN RESIDUAL STRENGTH vs NDI ESTIMATE OF CRACK LENGTH AT REAR OF HOLE (1)

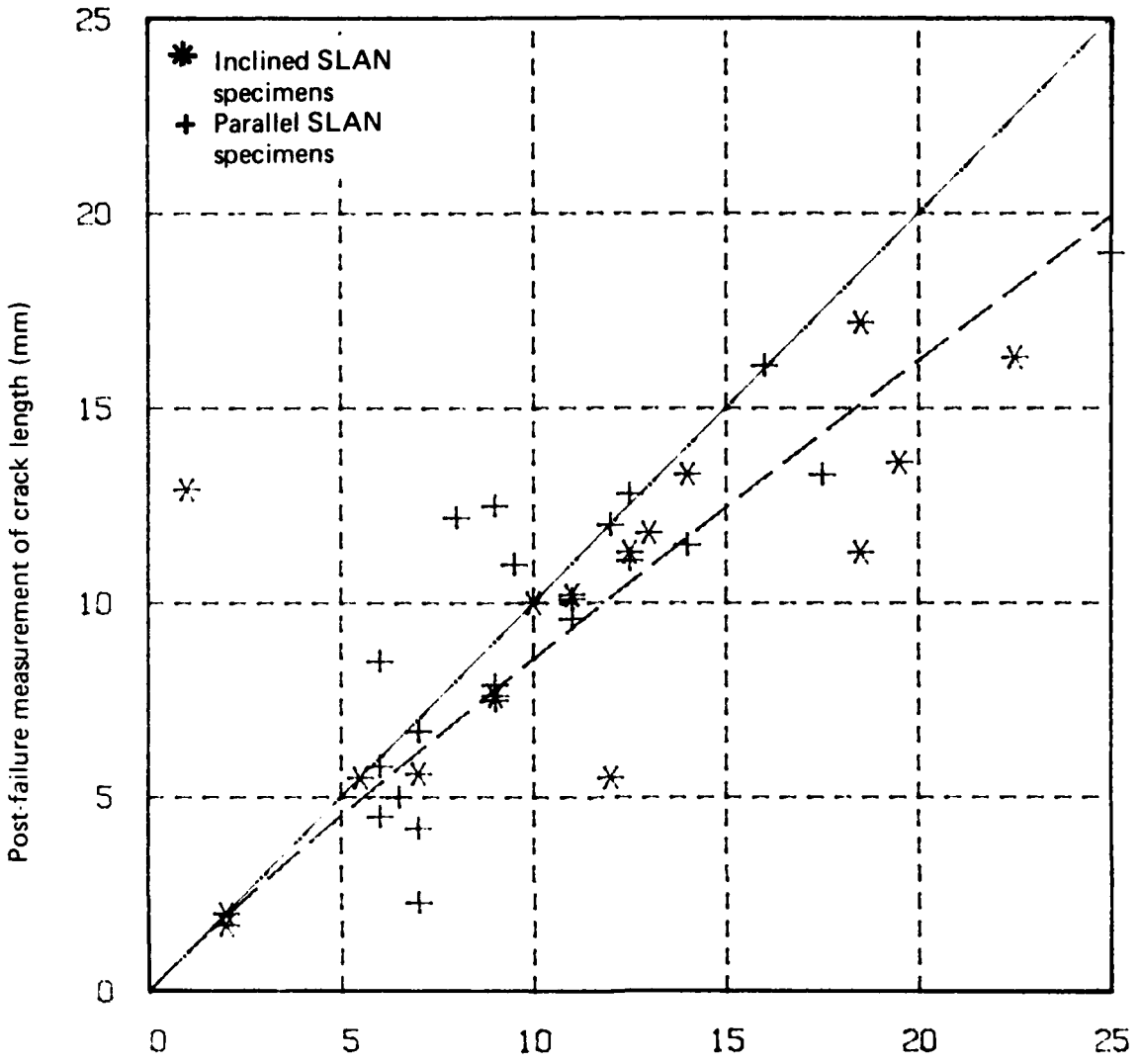

FIG. 11 ACCURACY OF CRACK LENGTH MEASUREMENTS USING FÖRSTER DEFECTOMAT EQUIPMENT

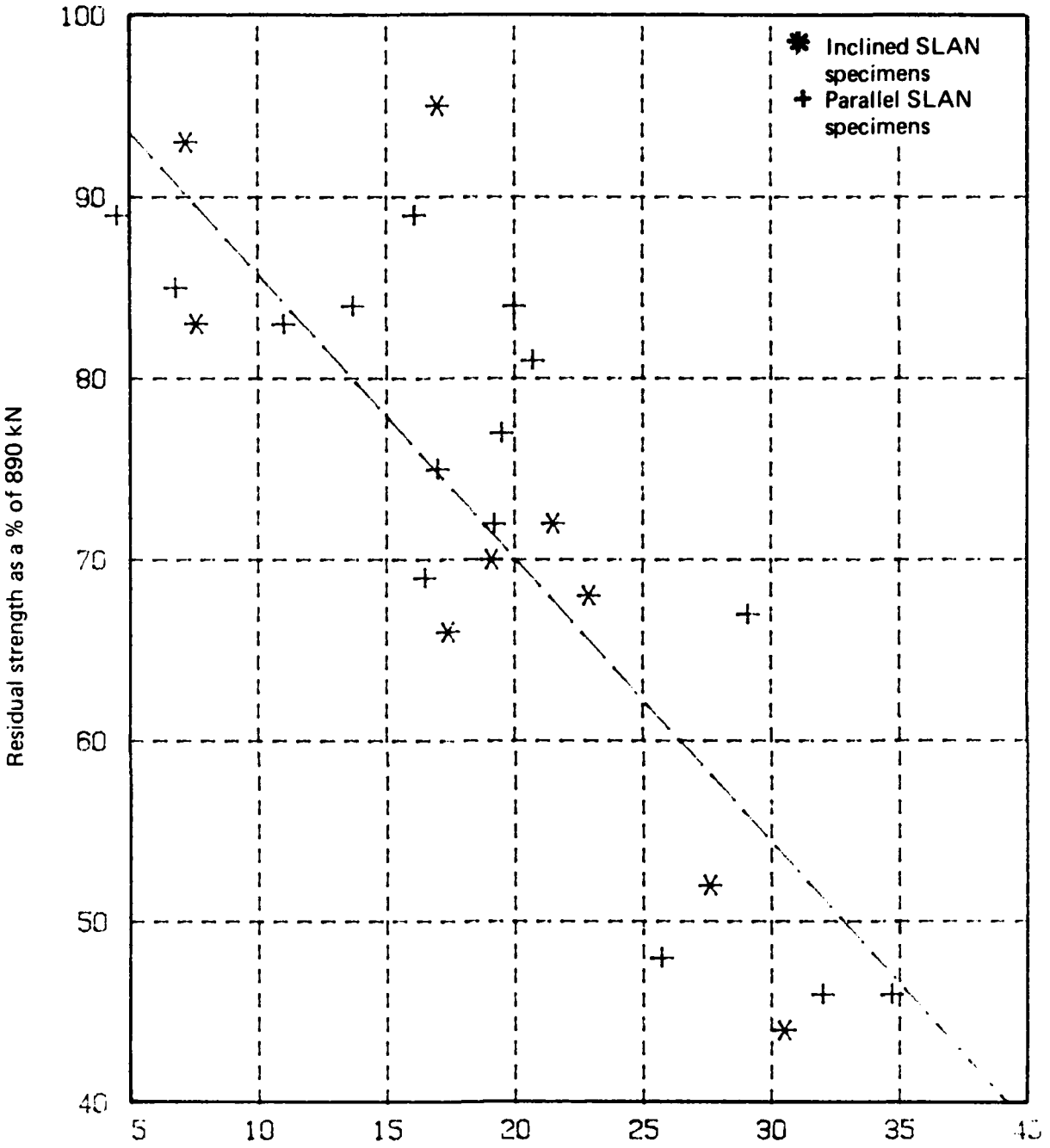

FIG. 12 SPECIMEN RESIDUAL STRENGTH vs SUM OF MEASURED CRACK LENGTHS FRONT AND REAR OF HOLE (1)

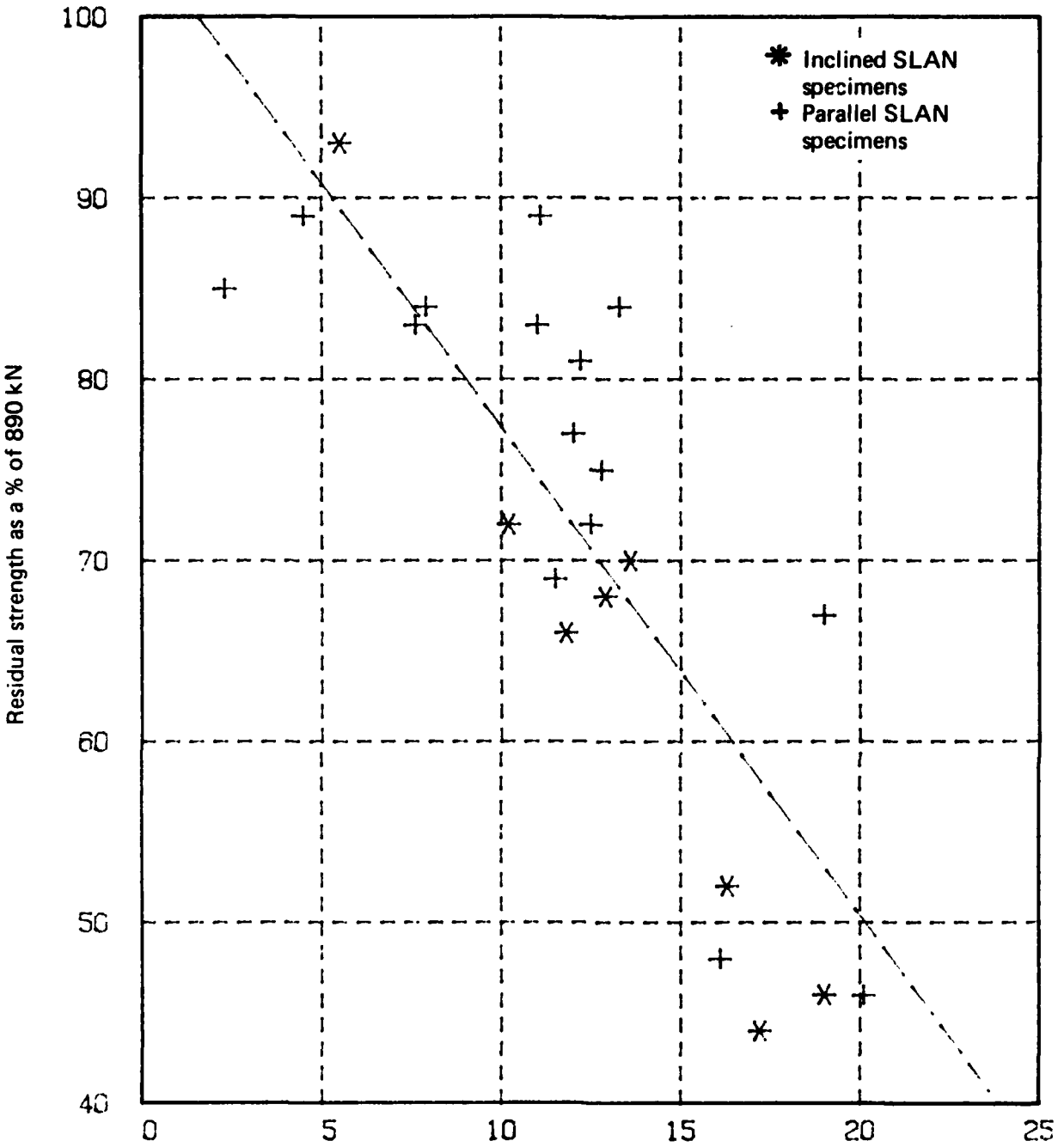

— — — 'Best fit' straight line

Residual strength = 104.3 – 2.69 (measured crack length)

r^2 = 0.67

FIG. 13 SPECIMEN RESIDUAL STRENGTH vs MEASURED CRACK LENGTH AT REAR OF HOLE (1)

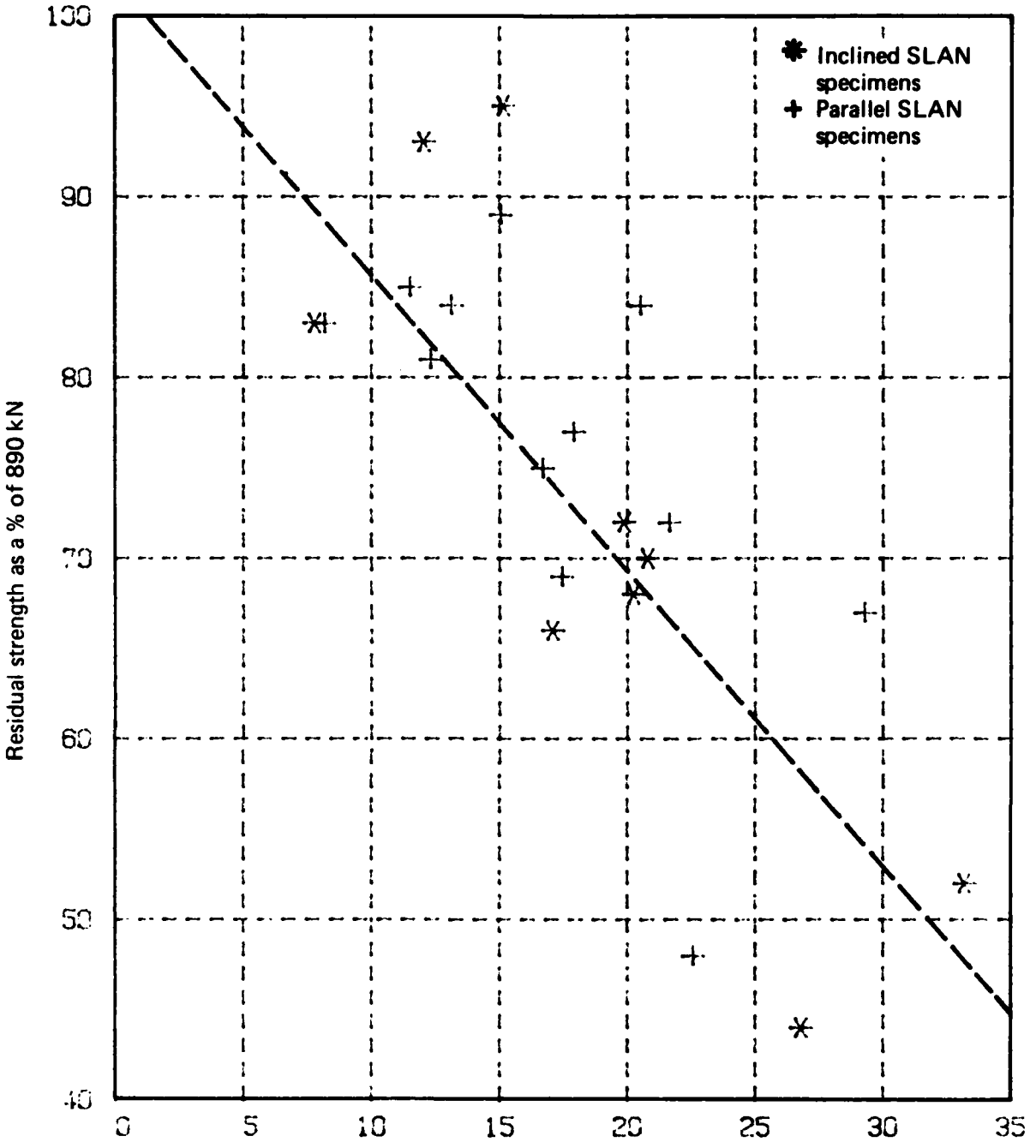

– – – – 'Best fit' straight line

Residual strength = 103.0 – 1.60 (sum of expected crack lengths)

r^2 = 0.57

FIG. 14 SPECIMEN RESIDUAL STRENGTH vs SUM OF EXPECTED ACTUAL CRACK LENGTHS FRONT AND REAR OF HOLE (1)

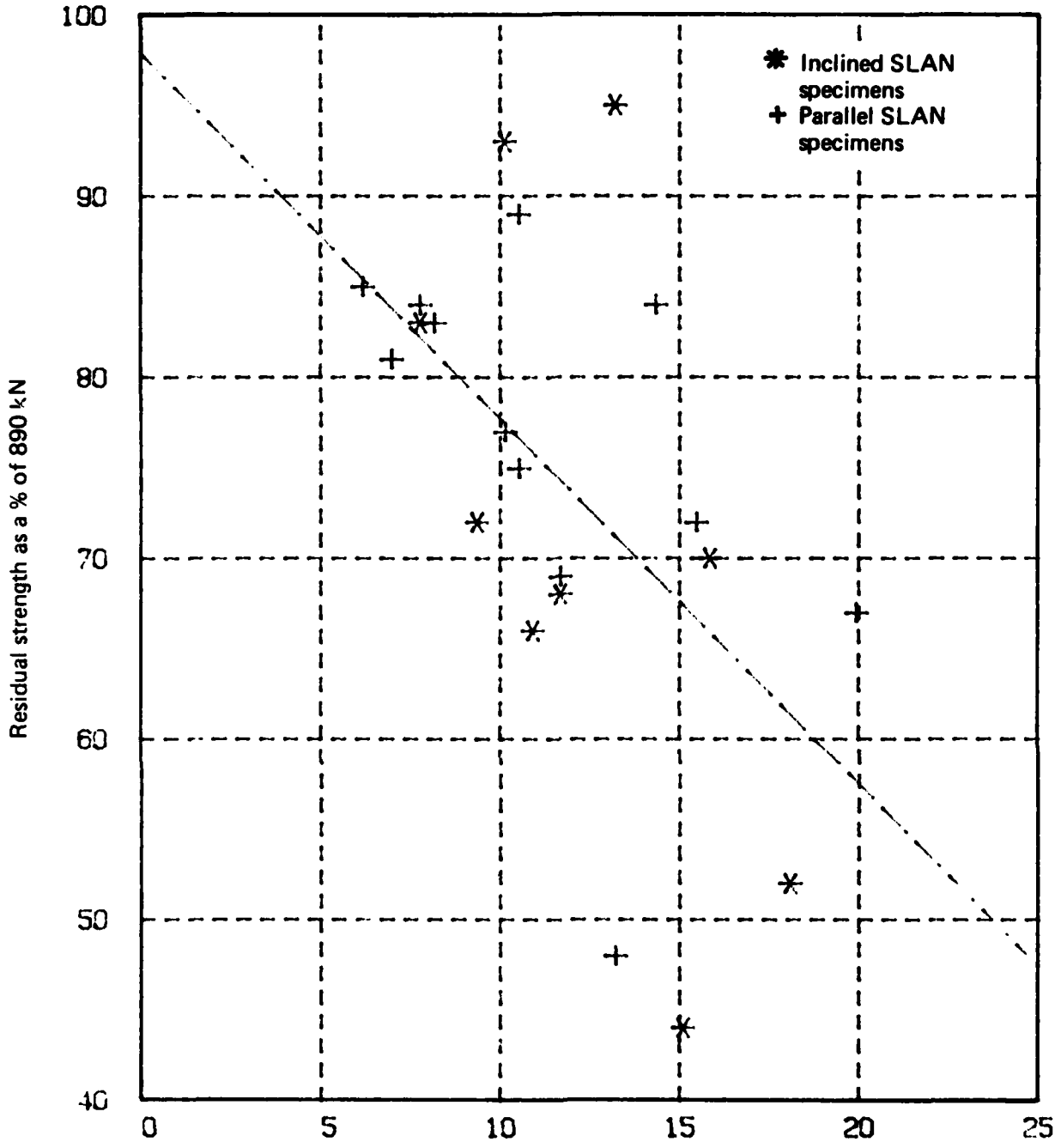

FIG. 15 SPECIMEN RESIDUAL STRENGTH vs EXPECTED ACTUAL CRACK LENGTH AT REAR OF HOLE (1)

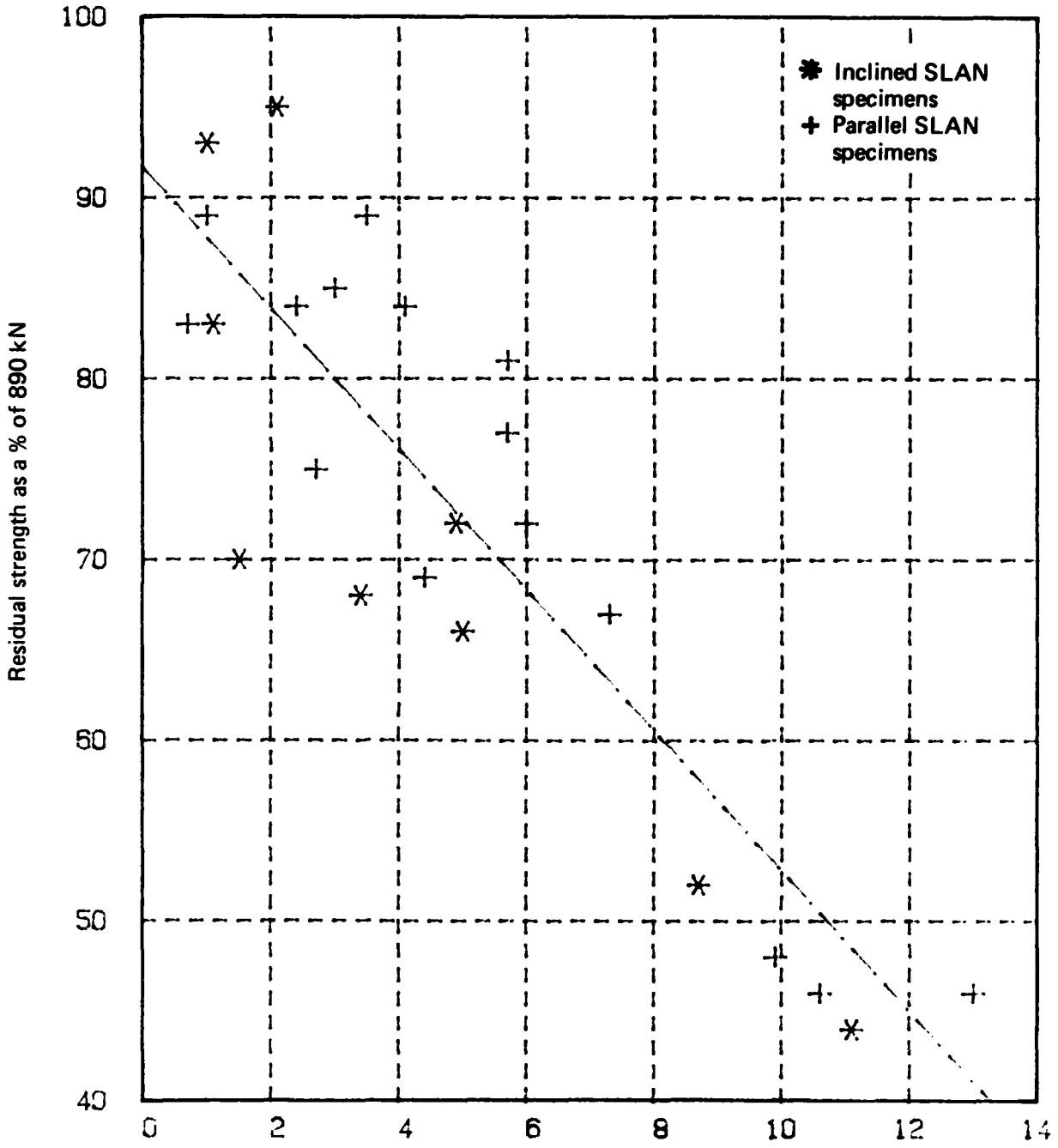

FIG. 16 SPECIMEN RESIDUAL STRENGTH vs SUM OF MEASURED CRACK DEPTHS FRONT AND REAR OF HOLE (1)

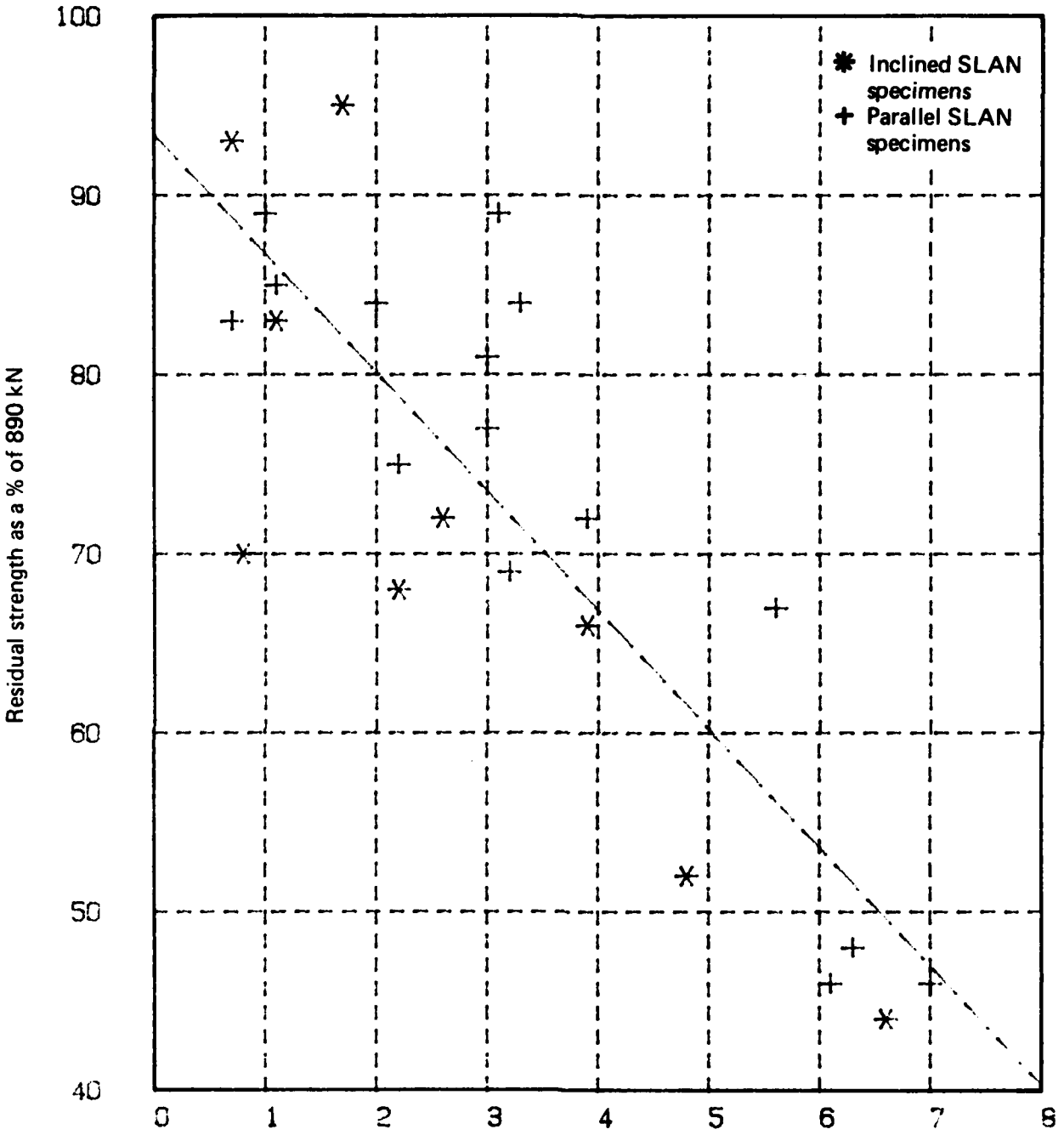

FIG. 17 SPECIMEN RESIDUAL STRENGTH vs MEASURED CRACK DEPTH AT REAR OF HOLE (1)

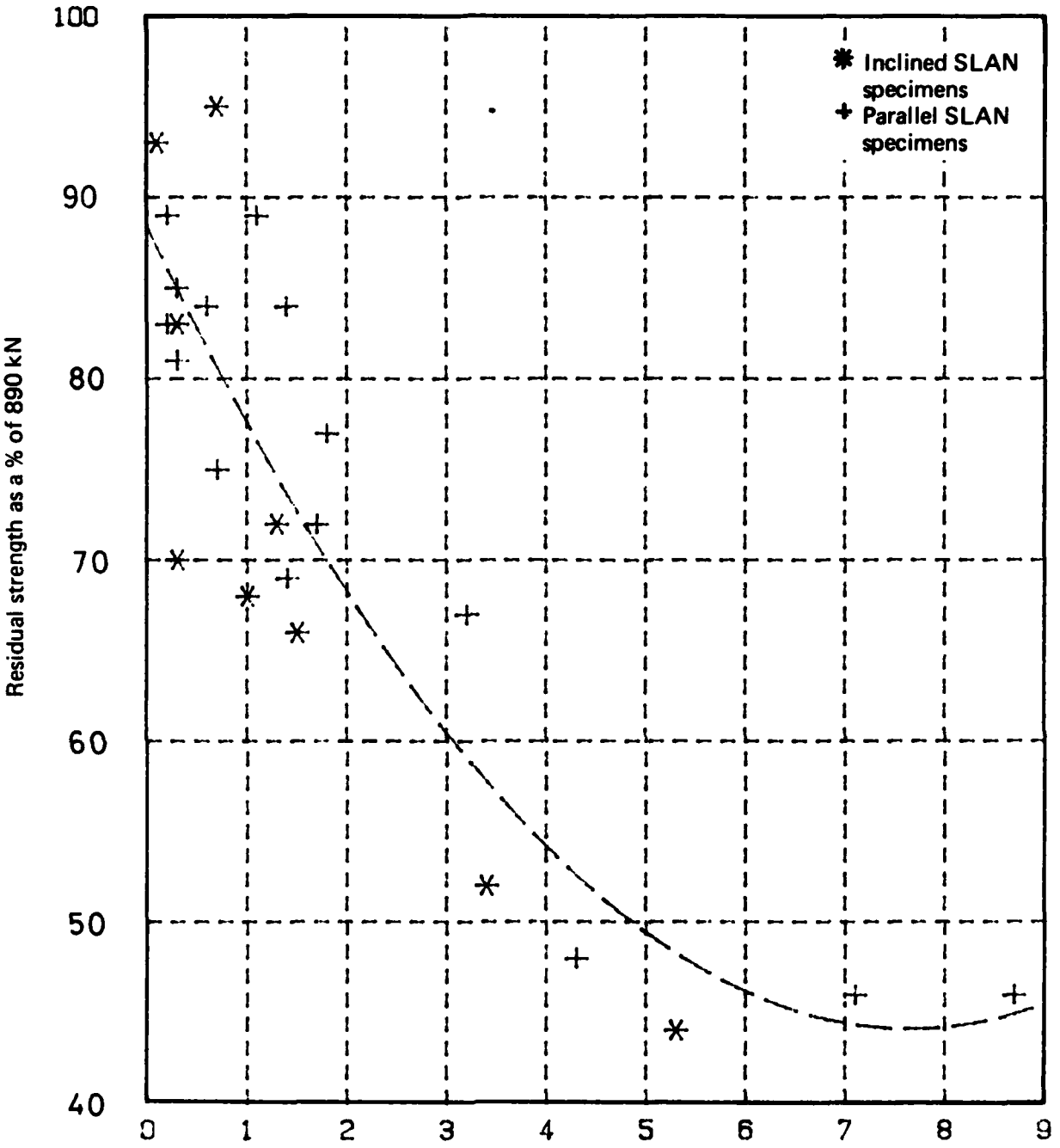

FIG. 18 SPECIMEN RESIDUAL STRENGTH vs SUM OF CRACKED AREAS FRONT AND REAR OF HOLE (1)

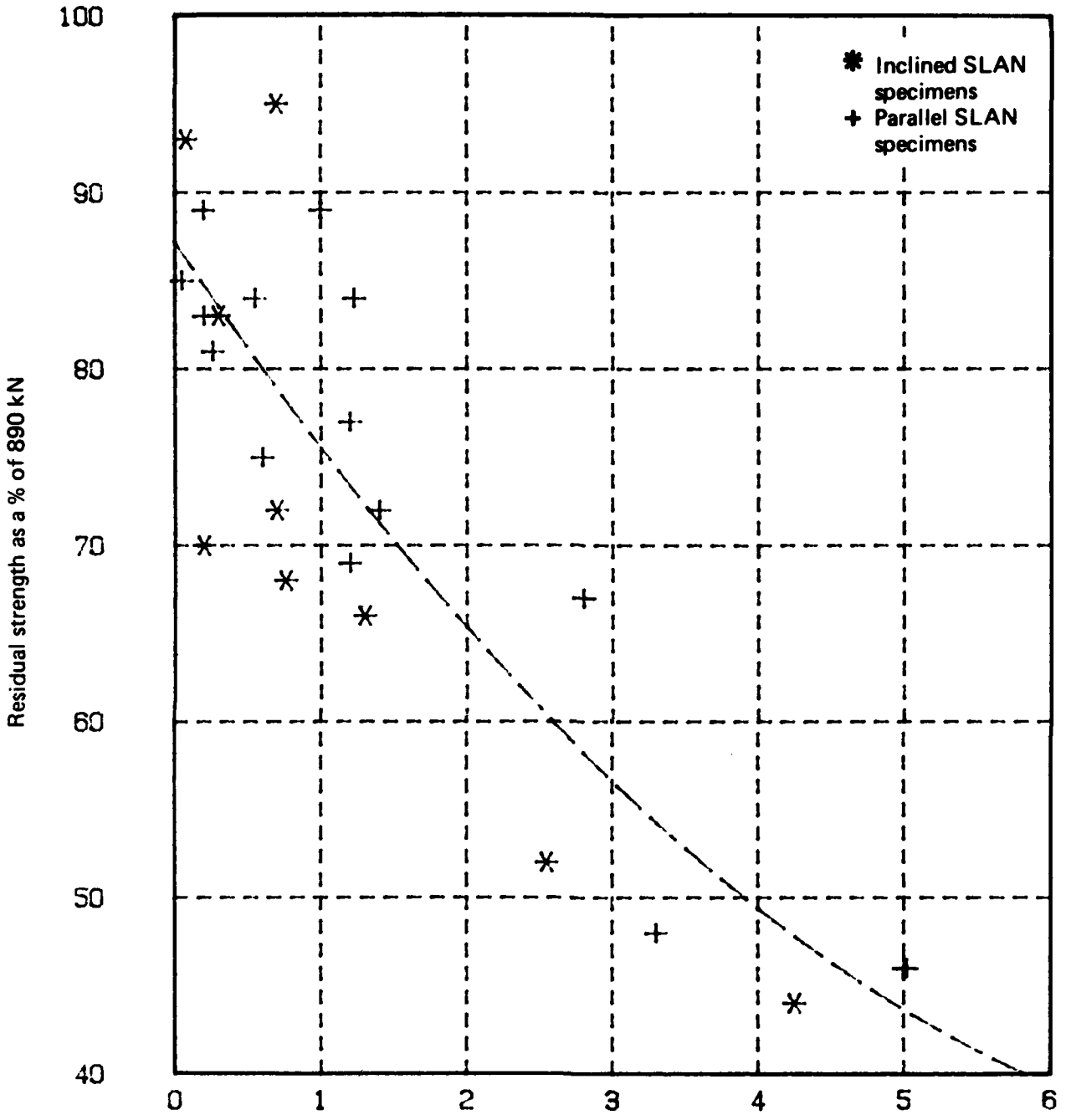

FIG. 19 SPECIMEN RESIDUAL STRENGTH vs CRACKED AREA AT REAR OF HOLE (1)

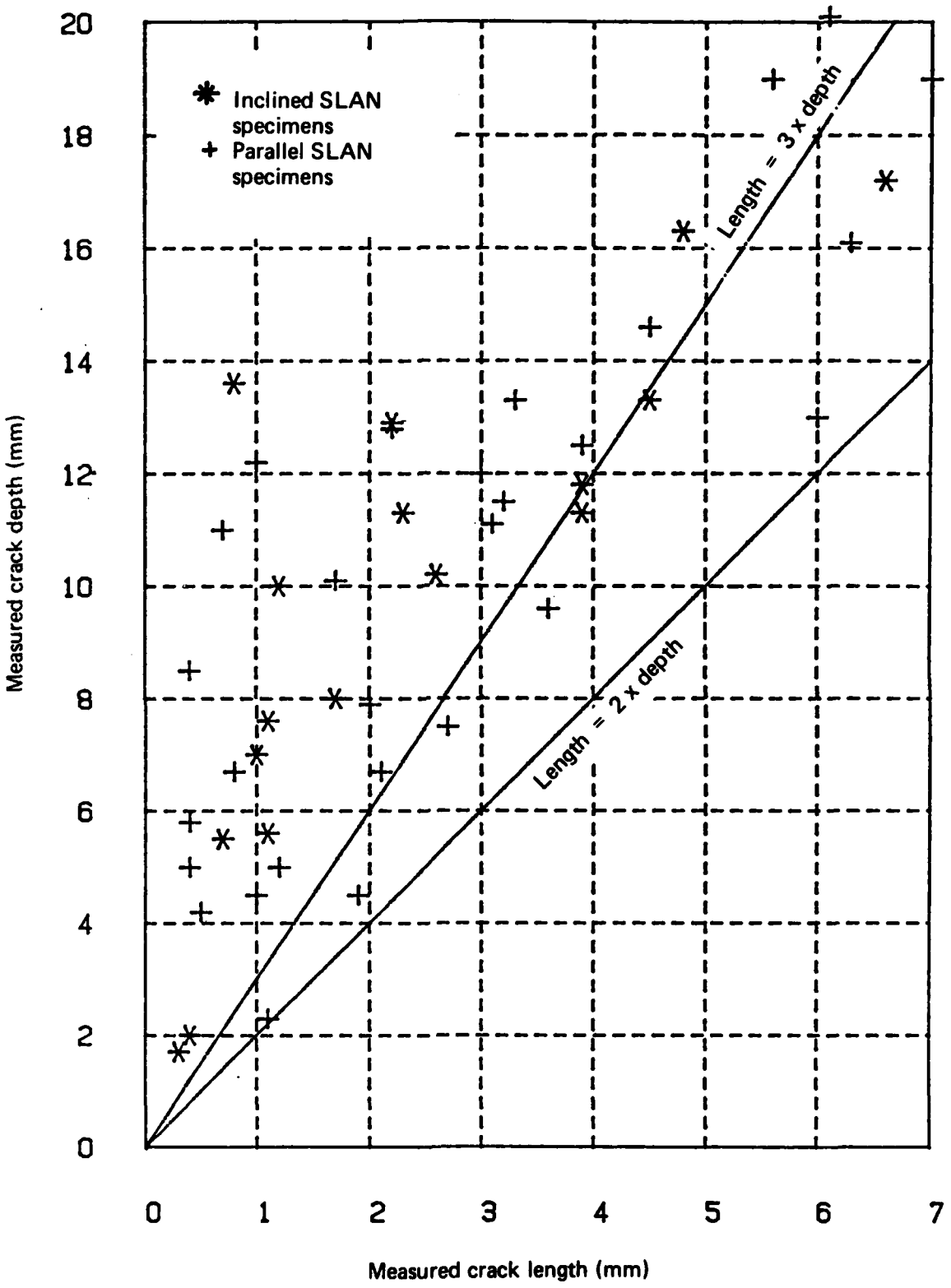

FIG. 20 MEASURED CRACK LENGTH vs MEASURED CRACK DEPTH AT HOLE (1)

DISTRIBUTION

AUSTRALIA

DEPARTMENT OF DEFENCE

Central Office

Chief Defence Scientist
Deputy Chief Defence Scientist
Superintendent, Science and Program Analysis
Controller, External Relations, Projects and Analytical Studies
} (1 copy)
Defence Science Adviser (U.K.) (Doc. Data sheet only)
Counsellor, Defence Science (U.S.A.) (Doc. Data sheet only)
Defence Science Representative (Bangkok)
Defence Central Library
Document Exchange Centre, D.I.S.B. (18 copies)
Joint Intelligence Organisation
Librarian H Block, Victoria Barracks, Melbourne
Director General—Army Development (NSO) (4 copies)

Aeronautical Research Laboratories

Director
Library
Divisional File—Structures
Superintendent—Materials
Author: A. S. Machin
R. A. Pell
G. S. Jost
G. W. Revill
B. C. Hoskin
J. M. Finney
L. M. Bland
C. K. Rider
J. M. Grandage
J. G. Sparrow
C. A. Patching
J. Y. Mann
W. F. Lupson
N. T. Goldsmith
B. C. Bishop

Materials Research Laboratories

Director/Library

Defence Research Centre

Library

Navy Office

Navy Scientific Adviser
Directorate of Naval Aircraft Engineering

Army Office

Army Scientific Adviser
Engineering Development Establishment, Library

Air Force Office

Air Force Scientific Adviser
Director General Aircraft Engineering—Air Force
HQ Support Command (SLENGO)
Air Attache Paris

DEPARTMENT OF DEFENCE SUPPORT

Government Aircraft Factories

Manager
Library

DEPARTMENT OF AVIATION

Library
Flying Operations and Airworthiness Division, Canberra, Mr C. Torkington

STATUTORY AND STATE AUTHORITIES AND INDUSTRY

CSIRO
  Materials Science Division, Library
Trans-Australia Airlines, Library
Qantas Airways Limited
SEC of Vic., Herman Research Laboratory, Library
Ansett Airlines of Australia, Library
B.H.P., Melbourne Research Laboratories
Commonwealth Aircraft Corporation
  Library
  Mr K. J. Kennedy (Manager Aircraft Factory No. 1)
  Manager Design Engineering
Hawker de Havilland Aust. Pty. Ltd., Bankstown, Library

CANADA

CAARC Coordinator Structures
International Civil Aviation Organization, Library
NRC
  Aeronautical & Mechanical Engineering Library

Universities and Colleges

Toronto — Institute for Aerospace Studies

FRANCE

ONERA, Library
AMD-BA
  M. M. Poyrony
  Mr D. Chaumette

INDIA

CAARC Coordinator Structures
Defence Ministry, Aero Development Establishment, Library
Hindustan Aeronautics Ltd., Library
National Aeronautical Laboratory, Information Centre

INTERNATIONAL COMMITTEE ON AERONAUTICAL FATIGUE

Per Australian ICAF Representative (25 copies)

ISRAEL

Israel Air Force
Israel Aircraft Industries
Technion-Israel Institute of Technology
Professor A. Buch

JAPAN

National Research Institute for Metals, Fatigue Testing Division
Institute of Space and Astronautical Science, Library

Universities

Kagawa University Professor H. Ishikawa

NETHERLANDS

National Aerospace Laboratory (NLR), Library

Universities

Technological University
of Delft Professor J. Schijve

NEW ZEALAND

Defence Scientific Establishment, Library
RNZAF, Vice Consul (Defence Liason)

SWEDEN

Aeronautical Research Institute, Library
Swedish National Defense Research Institute (FOA), Library

SWITZERLAND

Armament Technology and Procurement Group
F+W (Swiss Federal Aircraft Factory)
Dr H. Boesch
Mr A. Jordi

UNITED KINGDOM

Ministry of Defence, Research, Materials and Collaboration
CAARC, Secretary (NPL)
Royal Aircraft Establishment
Farnborough, Library
Commonwealth Air Transport Council Secretariat
National Engineering Laboratory, Library
British Library, Lending Division
CAARC Co-ordinator, Structures
Rolls-Royce Ltd.
Aero Division Bristol, Library
Welding Institute, Library
British Aerospace
Hatfield-Chester Division, Library
British Hovercraft Corporation Ltd., Library
Short Brothers Ltd., Technical Library

UNITED STATES OF AMERICA

NASA Scientific and Technical Information Facility
Applied Mechanics Reviews
Metals Information
The John Crerar Library
The Chemical Abstracts Service
Boeing Co.
Mr R. Watson
Mr J. C. McMillan
Lockheed-California Company
Lockheed Georgia
McDonnell Aircraft Company, Library
Nondestructive Testing Information Analysis Center

Universities and Colleges

Iowa	Professor R. I. Stephens
Illinois	Professor D. C. Drucker
Massachusetts Institute of Technology	M.I.T. Libraries

SPARES (15 copies)

TOTAL (161 copies)

Department of Defence

DOCUMENT CONTROL DATA

1. a. AR No.	1. b. Establishment No.	2. Document Date	3. Task No.
AR-003-942	ARL-STRUC-R-408	July 1984	DST 79/130

4. Title	5. Security	6. No. Pages
THE RESIDUAL STRENGTH OF CRACKED SPECIMENS REPRESENTING A SECTION OF THE MIRAGE IIIO WING MAIN SPAR	a. document: Unclassified b. title: U. c. abstract: U.	20 7. No. Refs: 7

8. Author(s)	9. Downgrading Instructions
A. S. Machin	—

10. Corporate Author and Address	11. Authority (*as appropriate*)
Aeronautical Research Laboratories P.O. Box 4331, Melbourne, Vic., 3001	a. Sponsor c. Downgrading b. Security d. Approval

12. Secondary Distribution (*of this document*)

Approved for public release

Overseas enquirers outside stated limitations should be referred through ASDIS, Defence Information Services Branch, Department of Defence, Campbell Park, CANBERRA, ACT, 2601.

13. a. This document may be ANNOUNCED in catalogues and awareness services available to . . .

No limitations

13. b. Citation for other purposes (*i.e. casual announcement*) may be (select) unrestricted (*or*) as for 13 a.

14. Descriptors		15. COSATI Group
Fracture strength	Fatigue (materials)	11130
Fracture (mechanics)		01030
Aluminium		
Cracking (fracturing)		
Eddy currents		
Nondestructive tests		

16. Abstract

The discovery of fatigue cracks at bolt holes in the wing main spar of many RAAF Mirage IIIO aircraft prompted an investigation into the residual strength of cracked specimens representing the critical section of the spar. Fatigue cracks were grown at the bolt holes of these specimens with frequent inspections to monitor the crack length. The specimens were then broken in static tension, the fracture surfaces photographed and the lengths, depths and areas of the fatigue cracks measured.

Using only the data available from the non-destructive inspection made just prior to the static failure it was not possible to accurately predict the specimen residual strength though it was possible to estimate a lower bound. Crack lengths as estimated by the NDI technique used were close to the measured crack lengths, though usually greater. Using the measured crack lengths, depths and areas it was not possible to accurately predict specimen residual strengths, though results were better than if information obtained only by NDI was used. Fracture mechanics

This page is to be used to record information which is required by the Establishment for its own use but which will not be added to the DISTIS data base unless specifically requested.

16. Abstract (*Contd*)

techniques could not be used to predict residual strengths because of a lack of suitable Stress Intensity factor solutions.

17. Imprint

Aeronautical Research Laboratories, Melbourne

18. Document Series and Number	19. Cost Code	20. Type of Report and Period Covered
Structures Report 408	251020	–

21. Computer Programs Used

22. Establishment File Ref(s)

END

FILMED

6-85

DTIC